p53 regulates expression of uncoupling protein 1 through binding and repression of PPAR coactivator-1

Hallenborg, Philip; Fjære, Even; Liaset, Bjørn; Petersen, Rasmus Koefoed; Murano, Incoronata; Sonne, Si Brask; Falkerslev, Mathias; Winther, Sally; Jensen, Benjamin Anderschou Holbech; Ma, Tao; Hansen, Jacob B; Cinti, Saverio; Blagoev, Blagoy; Madsen, Lise; Kristiansen, Karsten

Published in:
American Journal of Physiology: Endocrinology and Metabolism

DOI:
10.1152/ajpendo.00119.2015

Publication date:
2016

Document version
Version created as part of publication process; publisher's layout; not normally made publicly available

Citation for pulished version (APA):
Hallenborg, P., Fjære, E., Liaset, B., Petersen, R. K., Murano, I., Sonne, S. B., ... Kristiansen, K. (2016). p53 regulates expression of uncoupling protein 1 through binding and repression of PPAR coactivator-1. American Journal of Physiology: Endocrinology and Metabolism, 310(2), E116-E128. DOI: 10.1152/ajpendo.00119.2015

Articles in PresS. Am J Physiol Endocrinol Metab (November 17, 2015). doi:10.1152/ajpendo.00119.2015

p53 regulates expression of uncoupling protein 1 through binding and repression of PPARγ coactivator 1α

Philip Hallenborg[1,2], Even Fjære[2,3], Bjørn Liaset[3], Rasmus Koefoed Petersen[2], Incoronata Murano[4], Si Brask Sonne[2], Mathias Falkerslev[2], Sally Winther[2], Benjamin Anderschou Holbech Jensen[2], Tao Ma[2], Jacob B. Hansen[2], Saverio Cinti[4], Blagoy Blagoev[1], Lise Madsen[2,3], and Karsten Kristiansen[2,*]

1, Department of Biochemistry and Molecular Biology, University of Southern Denmark, 5230 Odense M, Denmark

2, Laboratory of Genomics and Molecular Biomedicine, Department of Biology, University of Copenhagen, 2200 Copenhagen N, Denmark

3, National Institute of Nutrition and Seafood Research, N-5817 Bergen, Norway.

4, Department of Experimental and Clinical Medicine, Center of Obesity Università Politecnica della Marche, via Tronto 10a, 60020 Ancona, Italy

**To whom correspondence should be addressed: Karsten Kristiansen, Laboratory of Genomics and Molecular Biomedicine, Department of Biology, University of Copenhagen, Universitetsparken 13, DK-2100 Copenhagen Ø, Denmark, Phone: +45 6011 2408, Fax: +45 3532 2128, Email: kk@bio.ku.dk*

Running title: *p53 inhibits UCP1 expression*

Keywords: p53, UCP1, PGC-1, adipose tissue

Background: Expression and activation of UCP1 in adipocytes increase energy expenditure through uncoupled respiration.

Results: Lack of p53 leads to increased expression of UCP1 in the inguinal white adipose tissue.

Conclusion: Through regulation of the coactivator function of PPARGC1a and PPARGC1b p53 modulates *Ucp1* expression in white adipose tissue.

Significance: Extends the growing list of metabolic processes regulated by the tumor suppressor p53.

ABSTRACT

The tumor suppressor p53 (TRP53 in mice) is known for its involvement in carcinogenesis, but work during recent years has underscored the importance of p53 in the regulation of whole body metabolism. A general notion is that p53 is necessary for efficient oxidative metabolism. The importance of UCP1-dependent uncoupled respiration and increased oxidation of glucose and fatty acids in brown or brown-like, termed BRITE or beige, adipocytes in relation to energy balance and homeostasis has recently been highlighted. UCP1-dependent uncoupled respiration in classic interscapular brown adipose tissue is central to cold-induced thermogenesis, whereas BRITE/beige adipocytes are of special importance in relation to diet-induced thermogenesis, where the importance of UCP1 is only clearly manifested in mice kept at

thermoneutrality. We challenged wildtype and TRP53-deficient mice by high fat feeding under thermoneutral conditions. Interestingly, mice lacking TRP53 gained less weight compared to their wildtype counterparts. This was related to an increased expression of *Ucp1* and other PPARGC1a and PPARGC1b target genes, but not *Ppargc1a* or *Ppargc1b* in inguinal white adipose tissue of mice lacking TRP53. We show that TRP53, independently of its ability to bind DNA, inhibits the activity of PPARGC1a and PPARGC1b. Collectively, our data shows that TRP53 has the ability to regulate the thermogenic capacity of adipocytes through modulation of PPARGC1 activity.

INTRODUCTION

Analyses of several genetically modified mouse models have during the last decades shown that predisposition to obesity can be regulated independently of food intake and physical activity (62). A large proportion of these mice show enhanced expression and/or activation of the uncoupling protein 1 (UCP1) (6). UCP1 functions as a proton channel in the inner mitochondrial membrane by-passing the normal ATP-production resulting in heat-production. Due to the possible beneficial effect of UCP1 in relation to the treatment of obesity, understanding its modes of function and regulation has been an area of intense interest.

The peroxisome proliferator-activated receptor γ coactivator 1α (PPARGC1a) plays a pivotal role in the control of *Ucp1* expression (35). Activation of this cofactor leads to the induction of not only *Ucp1* but also several genes involved in mitochondrial function including β-oxidation. The more recent family member, PPARGC1b, has been shown to share some, but not all functions with PPARGC1a in the regulation of the thermogenic program. However, complete attenuation of *Ucp1* expression in brown adipocytes requires ablation of both *Ppargc1a* and *Ppargc1b,* emphasizing an important role for PPARGC1a and PPARGC1b in controlling the expression of *Ucp1* (57). The ability of PPARGC1a to induce *Ucp1* expression is not limited to murine models as demonstrated by analysis of cells of human origin (3).

PPARGC1a was recently shown to act as a cofactor for the tumor suppressor p53, regulating the balance between cell cycle arrest and apoptosis downstream of p53-activation (54). Their interplay has also been emphasized by DePinho and colleagues showing TRP53-mediated regulation of *Ppargc1a* and *Ppargc1b* expression (51). p53 was for long regarded mainly as a dormant regulator of cell cycling and apoptosis activated in response to a variety of cellular stresses (26). However, an increasing number of articles has demonstrated a pivotal role for p53 as a regulator of metabolism in unstressed cells. Overall, data suggest that p53 supports oxidative metabolism (5). Notably, livers of mice deficient for TRP53 have lowered expression of synthesis of cytochrome c oxidase 2 (*Sco2*), which is essential for assembly of the mitochondrial cytochrome oxidase complex in the electron transport chain, and hence, oxidative metabolism (40).

It was recently reported that lack of TRP53 impaired expression of UCP1 and the development of interscapular brown adipose tissue, and accordingly, TRP53 was reported to protect mice against diet-induced obesity (43). Others and we have emphasized the importance of UCP1 expressing BRITE or beige adipocytes in white adipose depots in relation to protection against diet-induced obesity (38, 59). Of note, work by Cannon and Nedergaard has clearly demonstrated that the role of UCP1 in relation to diet-induced obesity is only observable when mice are kept at thermoneutral conditions (18).

Therefore, we decided to examine the phenotype of TRP53-deficient mice on a C57BL/6J background challenged with a high fat diet and kept under thermoneutral conditions.

Contrasting results obtained at room temperature by Rotter and coworkers (43), we observed that TRP53-deficient mice compared with wildtype mice were resistant to diet-induced obesity. Mice lacking TRP53 had augmented expression of *Ucp1* mRNA in their inguinal white adipose tissue. Furthermore, TRP53 could independently of its DNA-binding

ability repress the activity of PPARGC1a and thereby oxidative metabolism. Thus, our data suggest a tissue-specific involvement of TRP53 in its regulation of metabolism.

EXPERIMENTAL PROCEDURES

Cell culture and differentiation

Wildtype and TRP53-deficient mouse embryonic fibroblasts (MEFs) were generous gifts from Dr. Stephen N. Jones. MEFs were grown and differentiated as described elsewhere (24).

Plasmids

pCMVNeoBam-*Trp53* and -*Trp53 R175D* were generous gifts from Dr. Thierry Souissi. *Trp53* and *Trp53 R175D* were amplified using Primestar (Takara) according to manufacturer's instructions, inserted into pBluescript, sequenced, and moved into pBABE-puro (kindly granted by Dr. Ormond A. MacDougald). pBABE-puro TAg and pBABE-puro TAg K1 were described previously (23). TAg Δ was moved from pBABE-neo TAg Δ (kindly provided by Dr. Robert A. Weinberg) and insert into pBABE-puro. pCMX-*Gal4-Ppargc1a* was a generous gift from Dr. Dan Kelly. UASx4-TK luc was kindly supplied by Dr. Ronald M. Evans. Fragments of *Ppargc1a* were amplified by PCR using Primestar (Takara) and inserted into pGEX-5X-1 (GE Healthcare). pMD2.G, pMDLg/pRRE and pRSV-Rev were purchased from Addgene. pSicoR-lacZ, pSicoR-PPARGC1a I and pSicoR-PPARGC1a II were generous gifts from Dr. Susanne Mandrup.

Retro- and lentiviral transductions

Retroviral transduction was done as described previously with puromycin selection for two days (25). Lentiviral particles were produced as described (60). Lentiviral transduction was confirmed by inspection for GFP expression.

GST-pull down

Fusion proteins were expressed in *Escherichia coli* by induction with 0.1 mM isopropyl β-D-thiogalactosidase at 30 °C, cells were lysed by sonication, and incubated with Glutathione Sepharose (GE Healthcare). TRP53 was *in vitro* translated (TnT, Promega) in the presence of [^{35}S]-methionine (Amersham). Beads and *in vitro* translated proteins were incubated in pull down buffer (20 mM Tris-HCl, pH 8.0; 100 mM NaCl; 10 mM EDTA; 0.5% NP-40; 10 mM DTE; 1% skim-milk and protease inhibitors (Complete, Roche)) for 2 hours at 4 °C. Beads were washed once with pull-down buffer supplemented with skimmed milk and twice with pull-down buffer without skimmed milk, boiled in SDS-lysis buffer and resolved using SDS-PAGE. [^{35}S]-methionine-labelled proteins were visualized by autoradiography.

Fatty acid oxidation

Mitochondrial fatty acid oxidation was measured by $^{14}CO_2$ trapping from sealed culture flasks where medium was supplemented with 1-^{14}C-labelled palmitic acid (0.25 μCi/ml) and 500 μM L-carnitine as described elsewhere (4).

RNA purification, reverse transcription, and real-time PCR

RNA was purified using TRIzol (Invitrogen) according to manufacturer's instructions. Reverse transcription was performed essentially as described elsewhere (39). Quantitative PCR was performed in 25 µl reactions containing SYBR® Green JumpStart™ Taq ReadyMix™ (Sigma-Aldrich), 1.5 µl of diluted cDNA and 300 nM of each primer. Reaction mixtures were preheated at 95 °C for 2 min followed by 40 cycles of melting at 94 °C for 15 s, annealing at 60 °C for 30 s, elongation at 72 °C for 45 s. Primer sequences are available on request. Unless stated otherwise expression of TATA-box-binding protein (*Tbp*) mRNA was used for normalization.

Western blotting

Western blotting was performed as described previously (24). Primary antibody was UCP1 (Chemicon), TFIIB (Santa Cruz), Annexin II (Santa Cruz), TRP53 (Cell Signaling) and α-tubulin (Sigma-Aldrich). Secondary antibody was horseradish peroxidase-conjugated antibodies (DAKO). Quantification was done using the ImageJ software.

Isolation and culture of primary adipocytes

Primary brown (from interscapular, cervical and axillary BAT) and inguinal white pre-adipocytes from 6-7 weeks old TRP53 deficient male mice (B6.129-*Trp53*^{tm1Brd}N12, Taconic Biosciences) and corresponding wildtypes were isolated and cultured essentially as described elsewhere (8). Five weeks old mice were acclimated 1-2 weeks before they were sacrificed and used for isolation of adipose depots. After mincing the tissue was transferred to a HEPES-buffered solution (pH 7.4) containing 0.2% crude collagenase type II (Sigma-Aldrich) and digested at 37 °C for 30 min with constant shaking. The suspension was filtered (250-µm) and incubated on ice for 15 min to separate the mature adipocytes and the stromal vascular (SV) fraction. The SV fraction was then filtered through a 50-µm filter. Cells were pelleted (10 min, 700 G), resuspended in culture medium (DMEM, 4.5 g D-glucose/liter) (Sigma-Aldrich), 10% newborn calf serum (Life Technologies), 2.4 nM insulin (Novo Nordisk), 4 mM L-glutamine, 10 mM HEPES (Lonza), 25 µg/ml sodium ascorbate (Sigma-Aldrich), 50 IU/ml penicillin and 50 µg/ml streptomycin, centrifuged. resuspended in culture medium and plated in 6-well plates. Cultures were incubated in a humidified atmosphere of 8% CO_2 at 37 °C. Medium was changed 1, 3, 4 and 6 days after isolation. On day 4 and 6 the medium was supplemented with 500 nM rosiglitazone, and 5 ug/ml insulin. On day 8 the mature adipocytes were trypsinized, counted and replated in a gelatin coated seahorse plate.

Seahorse measurements

Two days after replating, real-time measurements of oxygen consumption rate (OCR) were performed using the Seahorse XF96 Extracellular Flux Analyzer (Seahorse Bioscience). One hour before the first measurement, the cell culture medium was changed to DMEM (Seahorse Bioscience) adjusted to 5 mM glucose (Sigma-Aldrich) and pH 7.4. OCR was measured under basal conditions and during successive adjustment to 1 µM isoproterenol (Sigma-Aldrich), 1 µM FCCP and a mixture of 1 µM rotenone and 1 µM antimycin A (Seahorse Bioscience).

Mice and feeding

In separate experiments, eight wildtype and eight *Trp53* null mice on a pure C57BL/6J background were purchased from either the Jackson Laboratory or Taconic Biosciences (strain designation B6.129S2-*Trp53*^{tm1Tyj}/J or B6.129-*Trp53*^{tm1Brd}N12, respectively). The mice were housed at thermoneutrality (28±2ºC), caged individually and fed either a regular chow or a high-fat diet (45% kcal fat, D12451, Research Diets) *ad libitum*. The feeding experiments were initiated when the mice were 9-10 weeks of age after acclimatization for 7 days in the animal facility. Feed intake was recorded three times a week and the mice were weighed once a week. After six weeks of feeding the mice were sacrificed by cardiac puncture under anesthesia (subcutaneous injection of 0.1 ml 1:1 Hypnorm:Dormicum per 10 grams of body weight). Blood was collected in tubes containing EDTA (Medinor AS, Oslo, Norway), centrifuged at 2500 g in 4°C for 5 min. Plasma was stored at -80°C until analyzed by commercial available enzymatic kits (Dialab, Vienne, Austria) using an autoanalyzer (MaxMat SA, Montpellier, France). Liver, muscle and adipose tissues were dissected out, weighed, snap-frozen in liquid nitrogen and stored at -80°C until further analyses. A portion of each adipose depot was fixed for histology. See histology section for further details. Glucose- and insulin tolerance tests were performed after 6h feed deprivation and in the fed state, respectively as described earlier (19) in a separate set of animals.

To examine the effect of housing temperature, three wild type mice and three *Trp53* null mice (strain designation B6.129-*Trp53*^{tm1Brd}N12) on a pure C57BL/6J background were purchased from Taconic Biosciences and fed a regular chow diet until 6 weeks of age. The mice were sacrificed by cervical dislocation. Interscapular brown adipose tissue was dissected out, snap-frozen in liquid nitrogen and stored at -80°C until further analyses.

Experiments were approved by the Animal Experiment Inspectorate in Denmark and the Norwegian Animal Research Authority in compliance with the European convention for the protection of vertebrate animals used for experiments and other scientific purposes (Council of Europe, no. 123, Strasbourg, France, 1985).

Indirect calorimetry

VO_2 and VCO_2 were measured in open-circuit indirect calorimetry cages as described previously (34). In short, the mice were housed in CaloCages (Phenomaster, TSE Systems). Measurements were performed for a total of 72h. The first 24h were regarded as an adaptation period and only the subsequent 48h were used for analyses.

Histological analyses

Sections of liver, inguinal white adipose tissue (iWAT), epididymal white adipose tissue (eWAT) and interscapular brown adipose tissue (iBAT) were fixed in 4% formaldehyde in 0.1 M phosphate buffer, pH 7.4 overnight, rinsed and stored in 0.1 M phosphate buffer, pH 7.4. Paraffin-embedded sections were stained with hematoxilin and eosin and/or incubated with UCP1 antibody according to standard procedures (11). Dewaxed sections were processed as follows: 1) hydrogen peroxide 0.3% in methanol for 30 min to block endogenous peroxidase; 2) normal rabbit serum (UCP1) 1:75 for 20 min to reduce nonspecific background staining; 3) sheep anti-rat antibody against UCP1 (kindly provided by Dr. D. Ricquier, Paris, France) diluted 1:3500 in PBS overnight at 4°C; 4) biotinylated secondary antibodies: rabbit anti-sheep IgG (UCP1) (Vector Laboratories; Burlingame, CA) 1:200 in PBS for 30 min; 5) ABC complex for 1 h (Vectastain ABC Kit, Vector Labs); 6) histochemical visualization of peroxidase using 3,3'-diaminobenzidine hydrochloride cromogen according to supplier's protocol (Sigma, St Louis, MO). Sections were counterstained with haematoxylin. The ability of the antibodies to specifically detect the antigens was evaluated in sections of tissues known to contain the antigens (such as the iBAT obtained from mice kept at 6°C for 10 days). Negative controls were obtained in each instance by omitting the primary antibody and using preimmune instead of primary antiserum

Adipocyte size was calculated as the mean adipocyte area of 200 random adipocytes in each section using a drawing tablet and the Nikon LUCIA IMAGE (version 4.61, Laboratory Imaging, Czech Republic) of the morphometric program. Tissue sections were observed with a Nikon Eclipse E800 light microscope using a x20 objective, and digital images were captured with a Nikon DXM 1200 camera.

The estimated, relative number of adipocytes in the epididymal white adipose stores was calculated by dividing the relative mass of the depot with the relative mass of individual adipocytes. This was estimated by converting the cell area into volume by assuming spherical shape of the adipocytes and similar density in wildtype and *Trp53*$^{-/-}$ mice.

Statistical analysis

Error bars represent standard error of the mean unless specified otherwise. Student's t-test was used unless stated otherwise to determine statistical significance. Each experiment was performed at least two independent times.

RESULTS

TRP53-deficient mice gain less weight than wildtype mice when fed a high-fat diet

We challenged mice harboring and lacking *Trp53* on a pure C57BL/6J background with either a regular chow or a high-fat diet under thermoneutral conditions. This mouse strain is highly susceptible to develop obesity and associated complications when fed excess calories. After 6 weeks of high fat feeding, TRP53-deficient mice on the high-fat diet were slimmer by macroscopic inspection and had gained significantly less body mass compared to their wildtype counterparts (Figure 1A+B). We observed no difference in the mice kept on chow. All mice used were 9-10 weeks of age at the onset of the experiment to avoid interference from possible tumor development in TRP53-deficient mice which happens at high rate later in life (14).

To verify that the reduced body mass gain in the high-fat fed mice was not simply due to reduced energy intake and/or reduced fat absorption, feed intake and stool fat content were measured. Interestingly, the fat content in stool from TRP53-deficient mice was lower than that in stool from wildtype mice (Figure 1C). As the feed intake was similar in the two groups of mice (Figure 1D), the decreased body mass gain indicated lowered feed efficiency in mice lacking TRP53 (Figure 1E).

Obesity is usually accompanied by decreased insulin sensitivity and impaired glucose homeostasis. The levels of serum glucose in the fed state were not statistically different between the two mice genotypes (Figure 1F). During the short feeding period, the absence of TRP53 did not affect glucose tolerance (Figure 1G). However, we did observe an increased glucose clearance in TRP53-deficient mice subjected to an insulin-tolerance test (Figure 1H) in agreement with previous findings (41) although there was no effect on the initial glucose disappearance rate (kITT) (wildtype: 1.76±0.40%/min and *Trp53-/-*: 2.82±0.92%/min, S.E.M.).

Surplus energy is stored as triglycerides in adipose tissues. Interestingly, the masses of adipose depots were decreased in mice lacking TRP53 but only in mice kept on the high-fat diet (Figure 2A).

The decreased mass of adipose depots could potentially be caused by defective adipogenesis in mice lacking TRP53. This assumption is, however, contradicted by the inhibitory effect of TRP53 on adipocyte differentiation reported by us and others (22, 43, 44). Furthermore, in keeping with *in vitro* findings, TRP53-deficient mice had an increased number of adipocytes in their adipose stores although the fat cells were smaller in size (Figure 2B-D) arguing against decreased adipogenesis in the TRP53-deficient mice.

During histological inspection of the white adipose stores, we furthermore observed decreased macrophage infiltration in the epididymal white adipose tissue (eWAT) of TRP53-deficient mice (Figure 2E). This finding was strengthened by decreased macrophage marker gene expression in the adipose stores of TRP53-deficient mice (Figure 2F). The decreased infiltration was in agreement with the improved ability of TRP53-deficient mice to cope with the high-fat feeding.

The lower adipose mass could then reflect impaired uptake of fatty acids in adipocytes, which presumably would lead to increased circulating levels and/or ectopic systemic deposition of fatty acids. Therefore, we measured the concentrations of triglycerides, free fatty acids, and glycerol in wildtype and TRP53-deficient mice. Plasma levels of triglycerides, free fatty acids, and glycerol were similar in mice of the both genotypes (Figure 1F). Furthermore, we observed no signs of steatosis in the livers of TRP53-deficient mice. Rather, histological examination revealed the presence of lipid droplets only in livers from wildtype mice (Figure 3A).

Fatty acids can be converted into ketone bodies in the liver. However, it is unlikely that the absence of steatosis in TRP53-deficient mice was caused by increased channeling of lipid into ketone body production as we found no significant difference in the plasma-level of OH-butyrate, the prime ketone body, between mice harboring or lacking TRP53 (Figure 1F). Furthermore, mRNA levels for the rate-limiting enzymes in ketone body production, acetyl-CoA acyltransferase 2 (*Acaa2*) and 3-hydroxy-3-methylglutaryl-CoA synthase 2 (*Hmgcs2*), were similar in mice of both genotypes (Figure 3B).

Collectively, these results show that at thermoneutrality TRP53-deficient mice were

protected against obesity and associated complications normally imposed by high-fat feeding.

Tissue-specific regulation of metabolic genes by TRP53

Rather than being stored, lipids can be catabolized in the adipose tissues through UCP1-dependent uncoupled respiration generating heat instead of ATP. This occurs in a subset of adipose stores, most notably in the brown adipose tissue (BAT) in relation to cold-induced thermogenesis, but accumulating evidence point to induction of UCP1 expression also in white depots as an important response to counteract diet-induced obesity (2, 38, 59).

We therefore speculated whether TRP53-deficient mice had altered expression of genes associated with thermogenesis. We found no differences in interscapular BAT (iBAT) (Figure 4A). This contrasted a recent report showing that TRP53 was required for normal iBAT development and UCP1 expression (43). However, these mice were not housed at thermoneutrality (V. Rotter, personal communication). To examine if housing temperature could underlay the different effects observed in response to *Trp53* ablation, we measured expression of *Ucp1* and other iBAT marker genes in wildtype and TRP53-deficient mice housed at 22ºC and kept on a chow diet. In contrast to the findings by Rotter and colleagues, *Ucp1* mRNA and UCP1 protein levels in iBAT were higher in mice lacking TRP53 indicating that a low sympathetic tone exacerbated UCP1 expression in the TRP53-deficient mice. Furthermore, expression of other iBAT marker genes was not impaired in the TRP-deficient mice (Figure 4B-D).

Interestingly, when assessing iWAT for expression of *Ucp1* and several other thermogenic markers, we found an upregulated expression of PPARGC1a and PPARGC1b target genes but neither *Ppargc1a* nor *Ppargc1b* mRNAs in mice lacking TRP53 compared to wildtype mice on a high-fat diet (Figure 5A). Of note, the increased *Ucp1* mRNA level in the iWAT of TRP53-deficient mice was accompanied with an augmented number of UCP1 protein immunoreactive multilocular cells with increased staining intensity (Figure 5B).

Furthermore, mice lacking TRP53 had increased expression in iWAT of genes encoding enzymes involved in β-oxidative pathways responsible for degradation of fatty acids, namely the carnitine palmitoyltransferases (*Cpt1a* (liver), *Cpt1b* (muscle and iWAT) and *Cpt2*), acyl-Coenzyme A dehydrogenase, medium chain (*Acadm*) and peroxisome proliferator-activated receptor α (*Ppara*). Interestingly, this increment was specific for the adipose tissue as their expression levels were unaltered in muscle and liver, two tissues with high β-oxidation capacity (Figure 5C).

We employed indirect calorimetry to investigate whether oxygen consumption, as would be predicted, was increased in the TRP53-deficient mice. However, no significant differences in oxygen consumption, CO_2 production or respiratory exchange ratio (RER) in TRP53-deficient mice were observed (Figure 6A-C), a result possibly reflecting that small changes in energy expenditure which over time significantly result in altered adipose mass cannot be determined by relative short-time indirect calorimetry measurements (7, 50, 56).

Collectively, these data indicate that energy expenditure is increased in TRP53-deficient mice, and that p53 regulates β-oxidative capacity in a tissue-specific manner. This notion was supported by the finding that the expression of Synthesis of Cytochrome c Oxidase 2, (*Sco2*) involved in mitochondrial respiration was similar in iWAT of wildtype and TRP53-deficient mice, but decreased in livers of mice lacking TRP53 (Figure 6D), the latter being in accordance with previous findings (40).

TRP53-deficient adipocytes express UCP1

The data above indicated that the ability of TRP53-deficient mice to resist high-fat feeding-induced obesity could rely at least partially on the increased activation of the thermogenic program in iWAT.

Mouse embryonic fibroblasts (MEFs) have been instrumental in deciphering adipocyte differentiation and function. We therefore speculated, if MEFs lacking TRP53 had increased propensity to express *Ucp1*. In agreement with earlier observations (22, 43, 44), MEFs lacking TRP53 had an augmented adipogenic potential (Figure 7A+B). Interestingly and in agreement with the *in vivo* findings, we observed a dramatic increase in *Ucp1* mRNA levels, but no differences in the expression of mRNAs encoding PPARGC1a and PPARGC1b in response to differentiation of MEFs with an adipogenic cocktail including rosiglitazone (Figure 7C). To compensate for differences in the degree of adipocyte differentiation between the TRP53-deficient and the wildtype MEFs, the expression levels of *Ucp1* mRNA and mRNAs encoding PPARGC1a and PPARGC1b were calculated relative to levels of mRNA encoding PPARγ2. The increment in *Ucp1* mRNA was accompanied by augmented expression levels of other genes associated with thermogenesis and known PPARGC1a and PPARGC1b target genes (Figure 7D) (13, 57).

A number of other adipose markers previously reported to characterize either white or brown adipocytes (53) were not specifically repressed or enriched, respectively, in TRP53-deficient adipocytes differentiated in the presence of rosiglitazone (Figure 7E) showing that the TRP53-deficient adipocytes did not resemble the classic interscapular brown adipocytes, suggesting that they more closely resemble BRITE/beige adipocytes.

Of note, inclusion of rosiglitazone during differentiation with the standard MDI cocktail of adipogenic inducers was necessary for induction of UCP1 in the MEF-derived TRP53-deficient adipocytes (Figure 7F).

Retinoic acids (RAs) and cAMP have previously been reported to augment *Ucp1* expression in brown adipocytes in cultures (11-13). We therefore examined if treatment with 9-cis RA and the cAMP elevating compound isoproterenol would be sufficient to induce *Ucp1* expression in the MEF-derived TRP53-deficient adipocytes. Interestingly, and in contrast to wildtype adipocytes, treatment of MDI-differentiated MEF-derived TRP53-deficient adipocytes with 9-cis RA and isoproterenol augmented *Ucp1* mRNA expression. This happened without an increase in the expression of mRNAs encoding PPARGC1a and PPARGC1b (Figure 8A). Still, expression of other PPARGC1a and PPARG1b target genes was also increased in the TRP53-deficient adipocytes upon 9-cis RA and isoproterenol treatment (Figure 8B).

SV40 large T antigen is known to bind and sequester various proteins including the retinoblastoma protein (pRB) and p53 (1). We have previously shown that ectopic expression of the TAg dramatically increased the expression of *Ucp1* in white adipocytes (23). We therefore sought to examine if inhibition of p53 was needed for the ability of TAg to induce *Ucp1* mRNA levels.

A mutant designated TAg K1 contains an amino acid substitution in the pRB consensus binding motif (LxCxE) and cannot bind to pRB family members whereas the TAg Δ (deletion 434-444) mutant holds a mutation in the bipartite p53-binding domain and cannot inactivate p53 (9, 32). In agreement with our earlier work (23), ectopic expression of Tag in both C3H10T1/2 cells and wildtype MEFs increased *Ucp1* mRNA expression, whereas expression of TAg K1 did not. Interestingly, although forced expression of TAg Δ did increase *Ppargc1a* mRNA levels, expression of *Ucp1* was not induced suggesting that p53 inactivation in this setting is necessary to increase *Ucp1* mRNA expression (Figure 9).

To further substantiate the negative impact of TRP53 on energy consumption in adipocytes, we isolated primary cells from iWAT as wells as iBAT depots from wildtype and TRP-deficient mice and differentiated them *in vitro*. We then assessed oxygen consumption and expression of several thermogenic and β-oxidative genes. Both basal and isoproterenol-stimulated oxygen consumptions were higher in cells from iWAT whereas only isoproterenol oxygen consumption was higher in primary adipocytes from iBAT (Figure 10A+C). Of note, chemical uncoupling by addition of FCCP increased oxygen consumption rate to the same level in both wildtype and TRP53-deficient adipocytes.

Thus, the FCCP-induced increase in oxygen consumption rate was less in the TRP53-deficient than in wildtype adipocytes, further demonstrating a higher level of uncoupled respiration in the TRP53-deficient adipocytes (Figure 10A+C) Reflecting the *in vivo* data, several genes involved in thermogenesis, mitochondrial electron transport, and β-oxidation were also upregulated in the *in vitro* differentiated iWAT-derived adipocytes lacking TRP53. However, in contrast to the *in vivo* results, expression of *Ppargc1a* and *Ppargc1b* mRNAs were higher in TRP53-deficient adipocytes than wildtype adipocytes, possibly reflecting a derepression the *Ppargc1a* and *Ppargc1b* promoters in the absence of p53 (51) in the setting of adipocytes differentiated from primary cells (Figure 10B+D). Furthermore, primary cells from iBAT also differentiated into adipocytes having higher expression of *Ucp1* mRNA, and mRNAs encoding proteins involved in mitochondrial electron transport (Figure 10D), suggesting a general adipocyte-related effect of p53. In this context it is noteworthy that expression of *Sco2* mRNA was not impaired in the *in vitro* differentiated primary adipocytes derived from iWAT or iBAT of TRP53-deficient mice (Figure 10B+D)

Collectively, our results indicate that the absence of p53 confers adipocytes with an increased ability to express UCP1.

p53 is a negative regulator of PPARG1a and PPARGC1b activity

Similar to iWAT of TRP53-deficient mice, MEF-derived *in vitro* differentiated adipocytes lacking TRP53 were able to augment *Ucp1* expression without a concomitant increase in the levels of mRNAs encoding PPARGC1a and PPARGC1b. Additionally, mutation of the p53 binding site in TAg prevented its ability to induce *Ucp1* expression despite augmented *Ppargc1* mRNA levels.

Still, we observed increased expression of genes previously shown to be regulated by PPARGC1a and PPARGC1b both during the rosiglitazone-induced differentiation of MEFs and by the 9-cis RA/isoproterenol treatment. The increased *Ucp1* levels in TRP53-deficient MEF-derived adipocytes might therefore occur independently of augmented expression of the *Ppargc1a* and *Ppargc1b*, suggesting that p53 apart from effects on the *Ppargc1a* (50) and possibly *Ppargc1b* promoters might directly repress the activity of PPARGC1a and PPARGC1b. Lentiviral shRNA-mediated knockdown of *Ppargc1a*, which also led to a decrease of *Ppargc1b* expression, showed that expression of *Ucp1* in the TRP53-deficient adipocytes was indeed dependent on the two cofactors (Figure 11A).

We therefore examined if p53 could modulate the activity of the cofactors directly. Not only was wildtype p53 able to decrease the activity of GAL4-fused PPARGC1a (Figure 11B). A DNA-binding deficient mutant (p53 R175D) also lowered PPARGC1a activity. The mutant was, however, less efficient despite similar levels of expression (Figure 10B). Furthermore, when performing GST-pull down with fragments of PPARGC1a, we were able to pull down *in vitro* translated p53. More specifically, p53 bound to two regions of PPARGC1a, aa202-403 and aa551-797 (Figure 11C).

If p53 regulates *Ucp1* expression independently of its DNA-binding ability, ectopic expression of the p53 R175D mutant should lower *Ucp1* mRNA levels in MEFs lacking TRP53 differentiated in the presence of rosiglitazone. Indeed, forced expression of p53 R175D lowered *Ucp1* mRNA expression (Figure 12A) showing that the ability of TRP53 to regulate expression of *Ucp1* was not dependent on its ability to bind DNA.

Besides regulating the expression of *Ucp1*, PPARGC1a and PPARGC1b are also involved in the regulation of several genes involved in oxidative phosphorylation in adipocytes (13, 57). In keeping with the suggested negative impact of p53 on PPARGC1a and PPARGC1b, ectopic expression of p53 R175D lowered both the expression levels of the rate-limiting enzymes in β-oxidation as well as β-oxidation itself in the TRP53-deficient adipocytes (Figure 12B+C).

Collectively, our data indicate that augmented activity of PPARGC1a and PPARGC1b contributed to the increased capacity of TRP53-deficient adipocytes to express *Ucp1*.

DISCUSSION

Albeit the tumor suppressor p53 has been most intensely studied in the context of cancer development, it is now acknowledged that p53 is involved in several aspects of metabolism (19). Here we expand the metabolic regulatory functions by showing that TRP53 can regulate *Ucp1* expression through inhibition of PPARGC1a and PPARGC1b activity. This interplay could, at least partly, explain the resistance to high-fat feeding-induced obesity of TRP53-deficient mice as these mice had increased levels of *Ucp1* in their iWAT. Although the augmented level of *Ucp1* expression in iWAT probably is an important contributor, it is likely that other systemic metabolic changes contribute to the high-fat resistant phenotype of TRP53-deficient mice. Defective oxidative metabolism in other organs, such as the liver, can augment the energy flux through futile cycles contributing to the metabolic inefficiency of these mice.

Surprisingly, our findings are contradictory to a recent article by Rotter and colleagues reporting that TRP53-deficient mice gained more weight compared with wildtype mice when challenged with a high-fat diet. This phenotype was explained by defective development of and UCP1 expression in the iBAT (43). This finding contrasts a previous study showing efficient differentiation of preadipocytes isolated from brown adipose tissue of TRP53-deficient mice. These adipocytes had high expression of UCP1 (28). In keeping with the latter report, we did not observe defects in neither iBAT appearances (data not shown) nor *Ucp1* expression in mice lacking TRP53 (Figure 4A). Furthermore, we did not observe impaired *in vitro* differentiation of cells from the stromal vascular fraction of iBAT of TRP53-deficient mice. Compared with *in vitro* differentiated adipocytes derived from the stromal vascular fraction isolated from wildtype mice, the TRP53-deficient adipocytes also exhibited higher expression of mRNAs encoding UCP1 and proteins involved in mitochondrial electron transport. Finally, reflecting the increased expression of these mRNAs, we were able to demonstrate increased oxygen consumption rate and higher levels of uncoupled respiration of *in vitro* differentiated adipocytes derived from the stromal vascular fraction of both iWAT and iBAT from TRP53-deficient mice compared to those derived from wildtype mice.

One possible explanation for these contradictory *in vivo* findings could be different housing temperatures since differences in housing temperatures previously have been shown to result in opposing findings examining UCP1-deficient mice (15, 18, 37). Thus, when housed at room temperature, UCP1-deficient mice do not gain weight relative to wildtype mice. However, when the mice are housed at thermoneutrality, the UCP1-deficient mice gained more weight than their wildtype counterparts (18). For this study, we housed mice at thermoneutrality (28 ºC) whereas in the study by Rotter the mice were kept at 22-23 ºC (Rotter, personal communication). It is difficult to explain how differences in housing temperatures could negatively affect the development of iBAT. However, in order to examine whether the divergent results could be due to different housing temperatures, we performed an additional experiment where wildtype and TRP53-deficient mice where housed at 22ºC. This experiment revealed that expression of *Ucp1* and other markers of iBAT was not impaired in mice lacking TRP53. Rather, expression of *Ucp1* mRNA and UCP1 was augmented in the TRP-deficient mice compared to wildtype mice.

Differences in mouse strains may affect the impact of TRP53 deficiency. Thus, it has been shown that the C57BL/6N strain differs with respect to several metabolic parameters from the C57BL/6J strain (55). However, in both studies C57BL/6J mice were used (Rotter, personal communication). Small difference may exist between the two lines used, but even so, it seems unlikely that such differences would explain the different results.

In our study, the mice were caged individually, whereas the mice used in the study of Rotter and

coworkers appeared to be co-caged except for the periods of measurements of food intake and detection of locomotor activity, where the mice were caged individually (43). Differences between co-caging and individual caging have been reported to affect physiological parameters likely to influence metabolic phenotypes (17, 20, 31).

Finally, recent publications have emphasized that the gut microbiota differs significantly between mice procured from different vendors and kept in different animal facilities (58, 63). Such differences in the gut microbiota may strongly influence the phenotype of genetically identical mice (58). Even though, differences in the composition of the gut microbiota may dramatically alter responses to high fat feeding, it is still difficult to explain how such differences should affect the developmental path leading to iBAT formation, also considering that iBAT is formed prenatally (10).

Despite augmented levels of *Ucp1* in the subcutaneous WAT and a robust decreased weight gain of TRP53-deficient mice, we observed no significant difference in the oxygen consumption between the mice. Still, *in vitro* differentiated primary adipocytes from TRP53-deficient mice had higher oxygen consumption. Minute changes in energy expenditure due to increased uncoupled respiration in subcutaneous WAT cannot be accurately determined during the relative short-time used for indirect calorimetry measurements. However, the cumulative effect of small changes in energy expenditure may over time result in decreased weight gain (7, 50, 56). But even so, it is unlikely that the expression of UCP1 in iWAT is the sole contributor to the obesity-resistant phenotype of the mice lacking *Trp53*.

Tissue-specific regulation of metabolic pathways may also play an important role. In this respect, it is interesting that p53 is a well-described regulator of lipid metabolism with the general assumption that p53 induces lipid catabolism (5, 21). Yet, we observed an inhibitory effect of TRP53 on fatty acid oxidation in adipocytes.

We find it conceivable that opposing effects on fatty acid handling in various tissues can result in a futile cycle where energy is lost rather than stored. To isolate the effect the contribution of adipose-p53 to whole body metabolism, it will be necessary to study the metabolic adaptability of a fat-specific knockout of *Trp53*.

The increased expression of *Ucp1* and genes involved in β-oxidation in the inguinal adipose depot in TRP53-deficient mice contrasts the previously reported decreased aerobic respiration in cells lacking p53 (7). These studies were performed in cancer cells or liver extracts. An indication that regulation of metabolism by p53 may be atypical in adipocytes was first reported by Finkel and colleagues showing that ablation of *Trp53* had a dramatic effect on the expression of the NAD-dependent deacetylase *Sirt1* only in adipose stores (45). SIRT1 regulates many aspects of metabolism, such as the response of adipocytes and hepatocytes to fasting (46, 49). Of note, *Ucp1* expression in TRP53-deficient adipocytes did not seem to be dependent on an increased SIRT1 activity, as the SIRT1 inhibitor nicotinamide had no effect on *Ucp1* mRNA levels (data not shown).

In keeping with the altered pattern of *Sirt1* regulation by TRP53 in adipose stores, differences in the regulation of *Sco2* by TRP53 exist between liver and adipocytes emphasizing that TRP53 exerts tissue specific effects on metabolism. Also, expression of other genes involved in metabolism previously shown to be regulated by TRP53 in other tissues was not significantly different in iWAT of mice lacking TRP53 (data not shown).

Our data indicate that the increased propensity of TRP53-deficient adipocytes to express *Ucp1* at least in part is the result of derepressed PPARGC1a (and PPARGC1b) activity and likely also related to a derepression of the *Ppargc1a* and *Ppargc1b* promoters. Of note, analyzing tissues, we observed the most pronounced effects in iWAT, whereas lack of TRP53 had little if any effect on expression of mRNAs encoding UCP1, PPARGC1a and PPARGC1b in iBAT in mice housed at thermoneutrality. In mice housed at 22ºC we however observed increased expression of UCP1 in iBAT of *Trp53*-deficient mice. TRP53 therefore

serves as an inhibitor UCP1 expression in iWAT and iBAT.

An inguinal specific positive effect on UCP1 expression has also recently been documented for PRDM16 (12, 52). In this respect, it is noteworthy that PRDM16 was suggested to augment PPARGC1a activity through replacing the corepressors C-terminal binding proteins (CtBPs) (30) with which p53 is known to interact (42). Expression of *Ppargc1a* and *Ppargc1b* mRNAs is higher in iBAT than in iWAT (36, 48). Conversely, TRP53 is more abundantly expressed in white compared to brown adipose tissue (29). It therefore seems possible that a balance between binding of PPARGC1a to p53-CtBP or PRDM16 in subcutaneous adipose depots could determine the level of UCP1 expression in these depots.

Interestingly, an association between p53 and PPARGC1a was shown to be important during glucose deprivation where PPARGC1a can act as a cofactor for TRP53 favoring the induction of genes regulating cell cycle arrest at the expense of apoptotic genes (54).

In transient transfection experiments wildtype p53 was more potent than a DNA-binding deficient mutant in repressing PPARGC1a activity (Figure 10B). It is possible that ectopically expressed wildtype TRP53 can recruit exogenous PPARGC1a to genomic DNA and thereby titrate it away from the artificial reporter. Other possible explanations include direct binding of wildtype TRP53 to the reporter plasmid or induction of an auxiliary protein facilitating the repression.

Besides direct association, it is possible that TRP53 controls PPARGC1a activity via other routes. The stability of PPARGC1a is regulated by the p38 MAPK (16, 47). TRP53 is known to affect the activity of the MAPK family (61). Altered p38 activity in the absence of TRP53 could therefore potentially contribute to the thermogenic phenotype of adipocytes lacking TRP53.

PPARG1a is also important for activation of gluconeogenesis in the liver (27, 65). Upon telomeric stress TRP53 can repress the expression of *Ppargc1a* and *Ppargc1b* leading to several defects including impaired gluconeogenesis in the liver (51). Contradictory to this suggested inhibitory effect of TRP53 on gluconeogenesis, starvation leads to lower blood glucose levels in TRP53-deficient mice compared with wildtype (45). This was suggested to be caused by defective starvation-induced expression of *Sirt1* in the liver of TRP53-deficient mice as SIRT1 is necessary for proper gluconeogenesis through modulation of PPARG1a activity (49).

It is therefore likely that both cell type and the mode of stress determine the outcome of the PPARGC1a-p53-SIRT1 interplay. During caloric overload associated with high-fat feeding, we observed similar expression levels of *Ppargc1a* and *Ppargc1b* mRNAs as well as mRNAs encoding the two rate-limiting enzymes in gluconeogenesis, phosphoenol-pyruvate carboxy-kinase (*Pck1*) and glucose 6-phosphatase (*G6pc*) in livers of wildtype and TRP53-deficient mice (data not shown). However, due to lack of reliable antibodies recognizing PPARGC1a and PPARGC1b we cannot entirely exclude the possibility that lack of TRP53 increases the level of the proteins, similar to the situation observed in RIP140-deficient cells (33).

Besides its role in regulation of *Ucp1* expression, TRP53 is involved in other aspects of adipocyte biology. Others and we observed increased levels of TRP53 in adipose stores of obese mice (Hallenborg et al., unpublished data) and (41, 64). This increased expression of TRP53 was recently suggested to contribute to adipocyte dysfunction during obesity by stimulating an inflammatory response through NF-κB (41). Based on the findings shown here, it is possible that augmented levels of p53 contribute to adipocyte dysfunction through inhibition of PPARGC1a and PPARG1b activity.

Its importance in mediating either cell cycle arrest or apoptosis upon DNA-damage has given p53 the nickname “Guardian of the Genome”. The recent findings emphasizing the role of p53 in regulation of metabolism suggest that p53 not only guards genome integrity but ensures that energy wasting is kept to a minimum.

REFERENCES

1. **Ali SH, and DeCaprio JA**. Cellular transformation by SV40 large T antigen: interaction with host proteins. *Semin Cancer Biol* 11: 15-23, 2001.
2. **Barbatelli G, Murano I, Madsen L, Hao Q, Jimenez M, Kristiansen K, Giacobino JP, De Matteis R, and Cinti S**. The emergence of cold-induced brown adipocytes in mouse white fat depots is determined predominantly by white to brown adipocyte transdifferentiation. *American journal of physiology Endocrinology and metabolism* 298: E1244-1253, 2010.
3. **Beranger GE, Karbiener M, Barquissau V, Pisani DF, Scheideler M, Langin D, and Amri EZ**. In vitro brown and "brite"/"beige" adipogenesis: human cellular models and molecular aspects. *Biochimica et biophysica acta* 1831: 905-914, 2013.
4. **Berge RK, Madsen L, Vaagenes H, Tronstad KJ, Gottlicher M, and Rustan AC**. In contrast with docosahexaenoic acid, eicosapentaenoic acid and hypolipidaemic derivatives decrease hepatic synthesis and secretion of triacylglycerol by decreased diacylglycerol acyltransferase activity and stimulation of fatty acid oxidation. *The Biochemical journal* 343 Pt 1: 191-197, 1999.
5. **Berkers CR, Maddocks OD, Cheung EC, Mor I, and Vousden KH**. Metabolic regulation by p53 family members. *Cell metabolism* 18: 617-633, 2013.
6. **Birerdinc A, Jarrar M, Stotish T, Randhawa M, and Baranova A**. Manipulating molecular switches in brown adipocytes and their precursors: a therapeutic potential. *Progress in lipid research* 52: 51-61, 2013.
7. **Burnett CM, and Grobe JL**. Dietary effects on resting metabolic rate in C57BL/6 mice are differentially detected by indirect (O2/CO2 respirometry) and direct calorimetry. *Molecular metabolism* 3: 460-464, 2014.
8. **Cannon B, and Nedergaard J**. Cultures of adipose precursor cells from brown adipose tissue and of clonal brown-adipocyte-like cell lines. *Methods Mol Biol* 155: 213-224, 2001.
9. **Chen S, and Paucha E**. Identification of a region of simian virus 40 large T antigen required for cell transformation. *J Virol* 64: 3350-3357, 1990.
10. **Cinti S, and Morroni M**. Brown adipocyte precursor cells: a morphological study. *Ital J Anat Embryol* 100 Suppl 1: 75-81, 1995.
11. **Cinti S, Zingaretti MC, Cancello R, Ceresi E, and Ferrara P**. Morphologic techniques for the study of brown adipose tissue and white adipose tissue. *Methods in molecular biology* 155: 21-51, 2001.
12. **Cohen P, Levy JD, Zhang Y, Frontini A, Kolodin DP, Svensson KJ, Lo JC, Zeng X, Ye L, Khandekar MJ, Wu J, Gunawardana SC, Banks AS, Camporez JP, Jurczak MJ, Kajimura S, Piston DW, Mathis D, Cinti S, Shulman GI, Seale P, and Spiegelman BM**. Ablation of PRDM16 and beige adipose causes metabolic dysfunction and a subcutaneous to visceral fat switch. *Cell* 156: 304-316, 2014.
13. **Cooper MP, Uldry M, Kajimura S, Arany Z, and Spiegelman BM**. Modulation of PGC-1 coactivator pathways in brown fat differentiation through LRP130. *The Journal of biological chemistry* 283: 31960-31967, 2008.
14. **Donehower LA, Harvey M, Slagle BL, McArthur MJ, Montgomery CA, Jr., Butel JS, and Bradley A**. Mice deficient for p53 are developmentally normal but susceptible to spontaneous tumours. *Nature* 356: 215-221, 1992.
15. **Enerback S, Jacobsson A, Simpson EM, Guerra C, Yamashita H, Harper ME, and Kozak LP**. Mice lacking mitochondrial uncoupling protein are cold-sensitive but not obese. *Nature* 387: 90-94, 1997.
16. **Fan M, Rhee J, St-Pierre J, Handschin C, Puigserver P, Lin J, Jaeger S, Erdjument-Bromage H, Tempst P, and Spiegelman BM**. Suppression of mitochondrial respiration through recruitment of p160 myb binding protein to PGC-1alpha: modulation by p38 MAPK. *Genes & development* 18: 278-289, 2004.

17. **Febinger HY, George A, Priestley J, Toth LA, and Opp MR**. Effects of housing condition and cage change on characteristics of sleep in mice. *Journal of the American Association for Laboratory Animal Science : JAALAS* 53: 29-37, 2014.
18. **Feldmann HM, Golozoubova V, Cannon B, and Nedergaard J**. UCP1 ablation induces obesity and abolishes diet-induced thermogenesis in mice exempt from thermal stress by living at thermoneutrality. *Cell metabolism* 9: 203-209, 2009.
19. **Fjaere E, Aune UL, Roen K, Keenan AH, Ma T, Borkowski K, Kristensen DM, Novotny GW, Mandrup-Poulsen T, Hudson BD, Milligan G, Xi Y, Newman JW, Haj FG, Liaset B, Kristiansen K, and Madsen L**. Indomethacin treatment prevents high fat diet-induced obesity and insulin resistance but not glucose intolerance in C57BL/6J mice. *The Journal of biological chemistry* 289: 16032-16045, 2014.
20. **Fuchsl AM, Langgartner D, and Reber SO**. Mechanisms underlying the increased plasma ACTH levels in chronic psychosocially stressed male mice. *PloS one* 8: e84161, 2013.
21. **Goldstein I, and Rotter V**. Regulation of lipid metabolism by p53 - fighting two villains with one sword. *Trends in endocrinology and metabolism: TEM* 23: 567-575, 2012.
22. **Hallenborg P, Petersen RK, Feddersen S, Sundekilde U, Hansen JB, Blagoev B, Madsen L, and Kristiansen K**. PPARgamma ligand production is tightly linked to clonal expansion during initiation of adipocyte differentiation. *Journal of lipid research* 2014.
23. **Hansen JB, Jorgensen C, Petersen RK, Hallenborg P, De Matteis R, Boye HA, Petrovic N, Enerback S, Nedergaard J, Cinti S, te Riele H, and Kristiansen K**. Retinoblastoma protein functions as a molecular switch determining white versus brown adipocyte differentiation. *Proceedings of the National Academy of Sciences of the United States of America* 101: 4112-4117, 2004.
24. **Hansen JB, Petersen RK, Larsen BM, Bartkova J, Alsner J, and Kristiansen K**. Activation of peroxisome proliferator-activated receptor gamma bypasses the function of the retinoblastoma protein in adipocyte differentiation. *The Journal of biological chemistry* 274: 2386-2393, 1999.
25. **Hansen JB, Zhang H, Rasmussen TH, Petersen RK, Flindt EN, and Kristiansen K**. Peroxisome proliferator-activated receptor delta (PPARdelta)-mediated regulation of preadipocyte proliferation and gene expression is dependent on cAMP signaling. *The Journal of biological chemistry* 276: 3175-3182, 2001.
26. **Harris SL, and Levine AJ**. The p53 pathway: positive and negative feedback loops. *Oncogene* 24: 2899-2908, 2005.
27. **Herzig S, Long F, Jhala US, Hedrick S, Quinn R, Bauer A, Rudolph D, Schutz G, Yoon C, Puigserver P, Spiegelman B, and Montminy M**. CREB regulates hepatic gluconeogenesis through the coactivator PGC-1. *Nature* 413: 179-183, 2001.
28. **Irie Y, Asano A, Canas X, Nikami H, Aizawa S, and Saito M**. Immortal brown adipocytes from p53-knockout mice: differentiation and expression of uncoupling proteins. *Biochemical and biophysical research communications* 255: 221-225, 1999.
29. **Kajimura S, Seale P, Kubota K, Lunsford E, Frangioni JV, Gygi SP, and Spiegelman BM**. Initiation of myoblast to brown fat switch by a PRDM16-C/EBP-beta transcriptional complex. *Nature* 460: 1154-1158, 2009.
30. **Kajimura S, Seale P, Tomaru T, Erdjument-Bromage H, Cooper MP, Ruas JL, Chin S, Tempst P, Lazar MA, and Spiegelman BM**. Regulation of the brown and white fat gene programs through a PRDM16/CtBP transcriptional complex. *Genes & development* 22: 1397-1409, 2008.
31. **Kalliokoski O, Teilmann AC, Jacobsen KR, Abelson KS, and Hau J**. The lonely mouse - single housing affects serotonergic signaling integrity measured by 8-OH-DPAT-induced hypothermia in male mice. *PloS one* 9: e111065, 2014.

32. **Kierstead TD, and Tevethia MJ**. Association of p53 binding and immortalization of primary C57BL/6 mouse embryo fibroblasts by using simian virus 40 T-antigen mutants bearing internal overlapping deletion mutations. *J Virol* 67: 1817-1829, 1993.

33. **Leonardsson G, Steel JH, Christian M, Pocock V, Milligan S, Bell J, So PW, Medina-Gomez G, Vidal-Puig A, White R, and Parker MG**. Nuclear receptor corepressor RIP140 regulates fat accumulation. *Proceedings of the National Academy of Sciences of the United States of America* 101: 8437-8442, 2004.

34. **Lillefosse HH, Tastesen HS, Du ZY, Ditlev DB, Thorsen FA, Madsen L, Kristiansen K, and Liaset B**. Hydrolyzed casein reduces diet-induced obesity in male C57BL/6J mice. *The Journal of nutrition* 143: 1367-1375, 2013.

35. **Lin J, Handschin C, and Spiegelman BM**. Metabolic control through the PGC-1 family of transcription coactivators. *Cell metabolism* 1: 361-370, 2005.

36. **Lin J, Puigserver P, Donovan J, Tarr P, and Spiegelman BM**. Peroxisome proliferator-activated receptor gamma coactivator 1beta (PGC-1beta), a novel PGC-1-related transcription coactivator associated with host cell factor. *The Journal of biological chemistry* 277: 1645-1648, 2002.

37. **Liu X, Rossmeisl M, McClaine J, Riachi M, Harper ME, and Kozak LP**. Paradoxical resistance to diet-induced obesity in UCP1-deficient mice. *The Journal of clinical investigation* 111: 399-407, 2003.

38. **Madsen L, Pedersen LM, Lillefosse HH, Fjaere E, Bronstad I, Hao Q, Petersen RK, Hallenborg P, Ma T, De Matteis R, Araujo P, Mercader J, Bonet ML, Hansen JB, Cannon B, Nedergaard J, Wang J, Cinti S, Voshol P, Doskeland SO, and Kristiansen K**. UCP1 induction during recruitment of brown adipocytes in white adipose tissue is dependent on cyclooxygenase activity. *PloS one* 5: e11391, 2010.

39. **Madsen L, Petersen RK, Sorensen MB, Jorgensen C, Hallenborg P, Pridal L, Fleckner J, Amri EZ, Krieg P, Furstenberger G, Berge RK, and Kristiansen K**. Adipocyte differentiation of 3T3-L1 preadipocytes is dependent on lipoxygenase activity during the initial stages of the differentiation process. *The Biochemical journal* 375: 539-549, 2003.

40. **Matoba S, Kang JG, Patino WD, Wragg A, Boehm M, Gavrilova O, Hurley PJ, Bunz F, and Hwang PM**. p53 regulates mitochondrial respiration. *Science* 312: 1650-1653, 2006.

41. **Minamino T, Orimo M, Shimizu I, Kunieda T, Yokoyama M, Ito T, Nojima A, Nabetani A, Oike Y, Matsubara H, Ishikawa F, and Komuro I**. A crucial role for adipose tissue p53 in the regulation of insulin resistance. *Nature medicine* 15: 1082-1087, 2009.

42. **Mirnezami AH, Campbell SJ, Darley M, Primrose JN, Johnson PW, and Blaydes JP**. Hdm2 recruits a hypoxia-sensitive corepressor to negatively regulate p53-dependent transcription. *Current biology : CB* 13: 1234-1239, 2003.

43. **Molchadsky A, Ezra O, Amendola PG, Krantz D, Kogan-Sakin I, Buganim Y, Rivlin N, Goldfinger N, Folgiero V, Falcioni R, Sarig R, and Rotter V**. p53 is required for brown adipogenic differentiation and has a protective role against diet-induced obesity. *Cell death and differentiation* 20: 774-783, 2013.

44. **Molchadsky A, Shats I, Goldfinger N, Pevsner-Fischer M, Olson M, Rinon A, Tzahor E, Lozano G, Zipori D, Sarig R, and Rotter V**. p53 plays a role in mesenchymal differentiation programs, in a cell fate dependent manner. *PloS one* 3: e3707, 2008.

45. **Nemoto S, Fergusson MM, and Finkel T**. Nutrient availability regulates SIRT1 through a forkhead-dependent pathway. *Science* 306: 2105-2108, 2004.

46. **Picard F, Kurtev M, Chung N, Topark-Ngarm A, Senawong T, Machado De Oliveira R, Leid M, McBurney MW, and Guarente L**. Sirt1 promotes fat mobilization in white adipocytes by repressing PPAR-gamma. *Nature* 429: 771-776, 2004.

47. **Puigserver P, Rhee J, Lin J, Wu Z, Yoon JC, Zhang CY, Krauss S, Mootha VK, Lowell BB, and Spiegelman BM**. Cytokine stimulation of energy expenditure through p38 MAP kinase activation of PPARgamma coactivator-1. *Molecular cell* 8: 971-982, 2001.

48. **Puigserver P, Wu Z, Park CW, Graves R, Wright M, and Spiegelman BM**. A cold-inducible coactivator of nuclear receptors linked to adaptive thermogenesis. *Cell* 92: 829-839, 1998.
49. **Rodgers JT, Lerin C, Haas W, Gygi SP, Spiegelman BM, and Puigserver P**. Nutrient control of glucose homeostasis through a complex of PGC-1alpha and SIRT1. *Nature* 434: 113-118, 2005.
50. **Rozman J, Klingenspor M, and Hrabe de Angelis M**. A review of standardized metabolic phenotyping of animal models. *Mammalian genome : official journal of the International Mammalian Genome Society* 25: 497-507, 2014.
51. **Sahin E, Colla S, Liesa M, Moslehi J, Muller FL, Guo M, Cooper M, Kotton D, Fabian AJ, Walkey C, Maser RS, Tonon G, Foerster F, Xiong R, Wang YA, Shukla SA, Jaskelioff M, Martin ES, Heffernan TP, Protopopov A, Ivanova E, Mahoney JE, Kost-Alimova M, Perry SR, Bronson R, Liao R, Mulligan R, Shirihai OS, Chin L, and DePinho RA**. Telomere dysfunction induces metabolic and mitochondrial compromise. *Nature* 470: 359-365, 2011.
52. **Seale P, Conroe HM, Estall J, Kajimura S, Frontini A, Ishibashi J, Cohen P, Cinti S, and Spiegelman BM**. Prdm16 determines the thermogenic program of subcutaneous white adipose tissue in mice. *The Journal of clinical investigation* 121: 96-105, 2011.
53. **Seale P, Kajimura S, Yang W, Chin S, Rohas LM, Uldry M, Tavernier G, Langin D, and Spiegelman BM**. Transcriptional control of brown fat determination by PRDM16. *Cell metabolism* 6: 38-54, 2007.
54. **Sen N, Satija YK, and Das S**. PGC-1alpha, a key modulator of p53, promotes cell survival upon metabolic stress. *Molecular cell* 44: 621-634, 2011.
55. **Simon MM, Greenaway S, White JK, Fuchs H, Gailus-Durner V, Wells S, Sorg T, Wong K, Bedu E, Cartwright EJ, Dacquin R, Djebali S, Estabel J, Graw J, Ingham NJ, Jackson IJ, Lengeling A, Mandillo S, Marvel J, Meziane H, Preitner F, Puk O, Roux M, Adams DJ, Atkins S, Ayadi A, Becker L, Blake A, Brooker D, Cater H, Champy MF, Combe R, Danecek P, di Fenza A, Gates H, Gerdin AK, Golini E, Hancock JM, Hans W, Holter SM, Hough T, Jurdic P, Keane TM, Morgan H, Muller W, Neff F, Nicholson G, Pasche B, Roberson LA, Rozman J, Sanderson M, Santos L, Selloum M, Shannon C, Southwell A, Tocchini-Valentini GP, Vancollie VE, Westerberg H, Wurst W, Zi M, Yalcin B, Ramirez-Solis R, Steel KP, Mallon AM, de Angelis MH, Herault Y, and Brown SD**. A comparative phenotypic and genomic analysis of C57BL/6J and C57BL/6N mouse strains. *Genome biology* 14: R82, 2013.
56. **Speakman JR**. Should we abandon indirect calorimetry as a tool to diagnose energy expenditure? Not yet. Perhaps not ever. Commentary on Burnett and Grobe (2014). *Molecular metabolism* 3: 342-344, 2014.
57. **Uldry M, Yang W, St-Pierre J, Lin J, Seale P, and Spiegelman BM**. Complementary action of the PGC-1 coactivators in mitochondrial biogenesis and brown fat differentiation. *Cell metabolism* 3: 333-341, 2006.
58. **Ussar S, Griffin NW, Bezy O, Fujisaka S, Vienberg S, Softic S, Deng L, Bry L, Gordon JI, and Kahn CR**. Interactions between Gut Microbiota, Host Genetics and Diet Modulate the Predisposition to Obesity and Metabolic Syndrome. *Cell metabolism* 22: 516-530, 2015.
59. **Vegiopoulos A, Muller-Decker K, Strzoda D, Schmitt I, Chichelnitskiy E, Ostertag A, Berriel Diaz M, Rozman J, Hrabe de Angelis M, Nusing RM, Meyer CW, Wahli W, Klingenspor M, and Herzig S**. Cyclooxygenase-2 controls energy homeostasis in mice by de novo recruitment of brown adipocytes. *Science* 328: 1158-1161, 2010.
60. **Ventura A, Meissner A, Dillon CP, McManus M, Sharp PA, Van Parijs L, Jaenisch R, and Jacks T**. Cre-lox-regulated conditional RNA interference from transgenes. *Proceedings of the National Academy of Sciences of the United States of America* 101: 10380-10385, 2004.
61. **Wu GS**. The functional interactions between the p53 and MAPK signaling pathways. *Cancer biology & therapy* 3: 156-161, 2004.
62. **Wu J, Cohen P, and Spiegelman BM**. Adaptive thermogenesis in adipocytes: is beige the new brown? *Genes & development* 27: 234-250, 2013.

63. **Xiao L, Feng Q, Liang S, Sonne SB, Xia Z, Qiu X, Li X, Long H, Zhang J, Zhang D, Liu C, Fang Z, Chou J, Glanville J, Hao Q, Kotowska D, Colding C, Licht TR, Wu D, Yu J, Sung JJ, Liang Q, Li J, Jia H, Lan Z, Tremaroli V, Dworzynski P, Nielsen HB, Backhed F, Dore J, Le Chatelier E, Ehrlich SD, Lin JC, Arumugam M, Wang J, Madsen L, and Kristiansen K**. A catalog of the mouse gut metagenome. *Nat Biotechnol* 2015.

64. **Yahagi N, Shimano H, Matsuzaka T, Najima Y, Sekiya M, Nakagawa Y, Ide T, Tomita S, Okazaki H, Tamura Y, Iizuka Y, Ohashi K, Gotoda T, Nagai R, Kimura S, Ishibashi S, Osuga J, and Yamada N**. p53 Activation in adipocytes of obese mice. *The Journal of biological chemistry* 278: 25395-25400, 2003.

65. **Yoon JC, Puigserver P, Chen G, Donovan J, Wu Z, Rhee J, Adelmant G, Stafford J, Kahn CR, Granner DK, Newgard CB, and Spiegelman BM**. Control of hepatic gluconeogenesis through the transcriptional coactivator PGC-1. *Nature* 413: 131-138, 2001.

FOOTNOTES

This work was supported by the Danish Natural Science Research Council, the Novo Nordisk Foundation, The Villum Foundation, The Lundbeck Foundation, the Carlsberg Foundation, and the EU FP7 project DIABAT (HEALTH-F2-2011-278373).

The authors declare no conflict of interests.

Abbreviations used are: eWAT, epididymal white adipose tissue; iBAT, interscapular brown adipose tissue; iWAT, inguinal white adipose tissue; MEF, mouse embryonic fibroblasts; PPARGC1a, peroxisome-proliferator activated receptor γ coactivator 1α; PPARGC1b, peroxisome-proliferator activated receptor γ coactivator 1β; PPARγ2, Peroxisome proliferator-activated receptor γ 2; RA, Retinoic acid; UCP1, Uncoupling protein 1.

FIGURE LEGENDS

FIGURE 1. Mice lacking TRP53 gain less weight when fed a high-fat diet. (A-C) Wildtype and TRP53-deficient mice were fed a chow or high-fat diet for 6 weeks. (A) Weight gain was assessed throughout the feeding period. (B) Picture of two representative mice on a high-fat diet. (C) Fat in feces measured by acid hydrolysis. (D) Weekly feed intake. (E) Relative feed efficiency calculated by dividing total weight gain with accumulated food intake. (F) Serum concentrations of metabolites. TG, triglyceride; FFA, free fatty acids; OH-butyrate, 4-hydroxy butyrate. (G) Glucose tolerance test. (H) Insulin tolerance test. (B, C, E, H) *, significance tested using student's *t*-test, $p < 0.05$.

FIGURE 2. Altered adipose phenotype of *Trp53*-deficient mice fed a high-fat diet. (A) Tissue weights in wildtype and *Trp53*-deficient mice kept on chow [C] or high-fat diet [H]. (B) Hematoxilin and eosin stainings of eWAT and iWAT from wildtype and *Trp53*-deficient mice. Bars correspond to 48 μm. (C) Average size of adipocytes in eWAT. (D) The estimated, relative number of adipocytes in eWAT in wildtype and *Trp53*-deficient mice. The approximation is based on assumed spherical shape and equal mass density. (E) Hematoxilin and eosin stainings of eWAT from wildtype and TRP53-deficient mice. Bars correspond to 24 μm. (F) Expression levels of the macrophage markers *Emr1 (*EGF-like module containing, mucin-like, hormone receptor-like sequence 1*)* and *Cd68*. (A, C, F) *, significance tested using student's *t*-test, $p < 0.05$.

FIGURE 3. Histological examination reveals fewer lipid droplets in livers from *Trp53*-deficient mice. (A) Hematoxilin and eosin staining of livers from wildtype and *Trp53*-deficient mice fed a high-fat diet. Bar corresponds to 48 μm. (B) mRNA levels of genes encoding ACAA2 and HMGCS2 were measured by real-time qPCR. *ACAA2*, acetyl-CoA acyltransferase 2. *HMGCS2*, 3-hydroxy-3-methylglutaryl-CoA synthase 2.

FIGURE 4. TRP53 is dispensable for iBAT development. (A) mRNA levels of thermogenic marker genes in iBAT of high-fat fed mice kept at thermoneutral conditions. *Cox8b*, cytochrome c oxidase, subunit VIII. *Dio2*, type II iodothyronine deiodinase. *Ppargc1a*, peroxisome proliferator-activated receptor γ coactivator-1α. *Ppargc1b*, peroxisome proliferator-activated receptor γ coactivator-1β *Ucp1*, uncoupling protein 1. *Pparg2*, peroxisome proliferator-activated receptor γ 2. (B) mRNA levels of thermogenic markers in iBAT of wildtype and Trp53-deficient mice housed at 22ºC. (C) Protein levels of UCP1 in iBAT of wildtype and TRP53-deficient mice

housed at 22ºC. Annexin II was included as loading control. (D) Quantification of western blots in (C). (B+D) *, significance tested using student's *t*-test, $p < 0.05$.

FIGURE 5. Increased expression of mRNA encoding UCP1 in inguinal white adipose tissue in mice lacking TRP53. (A) mRNA levels in inguinal, iWAT, adipose stores of thermogenic marker genes. *Cycs*, cytochrome c. *Prdm16*, PR domain containing 16. (B) Immunohistological examination of UCP1 expression in iWAT from wildtype and *Trp53*-deficient mice. (C) Expression of marker genes involved in β-oxidation in liver, muscle and iWAT from wildtype and *Trp53*-deficient mice fed a high-fat diet for 6 weeks. *Acadm*, acyl-Coenzyme A dehydrogenase, medium chain. *Cpt*, carnitine palmitoyltransferase. *Ppara*, peroxisome proliferator-activated receptor α. (A, D) *, significance tested using student's *t*-test, $p < 0.05$.

FIGURE 6. *Trp53*-deficient mice does not display measurable systemic alterations in respiration. (A+B) Indirect calorimetric measurements of O_2 consumption and CO_2 production of wildtype and TRP53-deficient mice fed a high-fat diet. (C) Respiratory exchange ratio (RER) on wildtype and TRP53-deficient mice on a high-fat diet. (D) mRNA levels of mRNA encoding SCO2 in livers and iWAT of wildtype and TRP53-deficient mice. SCO2, synthesis of cytochrome oxidase 2. *, significance tested using student's *t*-test, $p < 0.05$.

FIGURE 7. *Trp53*-deficient adipocytes have increased propensity to express *Ucp1*. Wildtype and TRP53-deficient fibroblasts were induced to undergo adipogenesis in the presence of rosiglitazone. Differentiation was evaluated by Oil-Red-O staining of triglycerides (A) or adipocyte marker gene expression by real-time qPCR (B). (C-E) Gene expression analyses by real-time qPCR normalized to *Pparγ2* mRNA to compensate for differences in degree of differentiation. mRNA expression levels of *Ucp1*, *Ppargc1a* and *Ppargc1b* (C), *Dio2*, *Cycs*, *Cox8b*, *Cox7a1* and *Cidea* (D) as well as the white and brown adipocyte marker genes (E). *Psat*, Phosphoserine aminotransferase. *Serpina3k*, Serine protease inhibitor A3K. *Prdm16*, PR domain containing 16. *Otop1*, otopetrin-1. *Eva1*, protein Eva-1 homolog. *Ntrk3*, NT-3 growth factor receptor. (F) Wildtype and TRP53-deficient fibroblasts were induced to undergo adipogenesis in the presence or absence of rosiglitazone. Level of UCP1 was determined by western blotting. TFIIB served as loading control. (B-E) Error bars represent standard deviation. *, significance tested using student's *t*-test, $p < 0.05$.

FIGURE 8. Retinoic acid and a β-adrenergic agonist induce *Ucp1* expression in TRP53-deficient adipocytes. Wildtype and TRP53-deficient MEFs were differentiated in the absence of rosiglitazone and stimulated with isoproterenol and 9-cis retinoic acid (9cis+Isoprot) for 24 hours. Shown is induction of *Ucp1*, *Ppargc1a* and *Ppargc1b* mRNAs (A) as well as *Dio2*, *Cycs*, *Cox8b*, *Cox7a1* and *Cidea* mRNAs (B). (A, B) Error bars represent standard deviation. *, significance tested using student's *t*-test, $p < 0.05$.

FIGURE 9. TAg deficient in p53 binding increased expression of *Ppargc1a* but not *Ucp1*. C3H10T1/2 (A) and wildtype MEFs (B) were transduced with virus encoding wildtype or mutants versions of TAg, selected and differentiated. Expression of *Ucp1*, *Ppargc1a* and *Fabp4* was determined by real-time qPCR. a, b, significance tested using one-way ANOVA, $p < 0.05$.

FIGURE 10. ***In vitro*** **differentiated primary adipocytes lacking** ***Trp53*** **have higher oxygen consumption and expression of genes involved in thermogenesis and β-oxidation.** Primary cells from iWAT (A+B) and iBAT (C+D) from wildtype and *Trp53-/-* mice were differentiated into adipocytes. (A+C) Oxygen consumption was measured using a Seahorse XF Analyzer. Cells were treated with isoproterenol (I), the uncoupling agent FCCP (II) and the inhibitors of the electron transport chain antimycin A+rotenone (III). Oxygen consumption rate is depicted relative to levels in cells treated with antimycin A+rotenone. (B+D) mRNA levels of genes involved in thermogenesis and β-oxidation were determined by real-time qPCR. *, significance tested using student's t-test, $p < 0.05$.

FIGURE 11. p53 decreases the activity of PPARGC1a (A) TRP53-deficient MEFs were lentivirally transduced with vectors expressing shRNA against *lacZ* or *Ppargc1a*, differentiated in the presence of rosiglitazone and expression of *Ucp1*, *Ppargc1a* and *Ppargc1b* mRNAs was measured used real-time qPCR. Error bars represent standard deviation. a, b, c, significance tested using one-way ANOVA, $p < 0.05$. (B) TRP53-deficient MEFs were transfected with UAS-GAL luciferase-reporter, a vector expressing GAL4-fused to PPARGC1a and either empty vector, or different amounts of vectors expressing wildtype p53 or the DNA-binding deficient mutant p53 R175D. Luciferase activity was normalized to β-galactosidase activity. Expression of p53 is shown by Western blotting below columns. α-tubulin served as loading control. a, b, c, d, significance tested using one-way ANOVA, $p < 0.05$. (C) GST-pull down of *in vitro* translated p53 using GST alone or GST fused to PPARGC1a fragments. Input represents 2 % of added *in vitro* reaction.

FIGURE 12. Ectopic expression of DNA-binding deficient p53 lowers ***Ucp1*** **expression and β-oxidative capacity of TRP53-deficient adipocytes.** TRP53-deficient MEFs were transduced with empty vector or a vector expressing p53 R175D, and differentiated in the presence of rosiglitazone. Levels of mRNA encoding UCP1 (A) or the β-oxidative enzymes CPT1b, CPT2, ACADM and PPARα (B) were measured using real-time qPCR. Error bars represent standard deviation. (C) β-oxidation in the differentiated, transduced cells. Levels of β-oxidation were assessed by conversion of palmitate to CO_2. *, significance tested using student's *t*-test, $p < 0.05$.

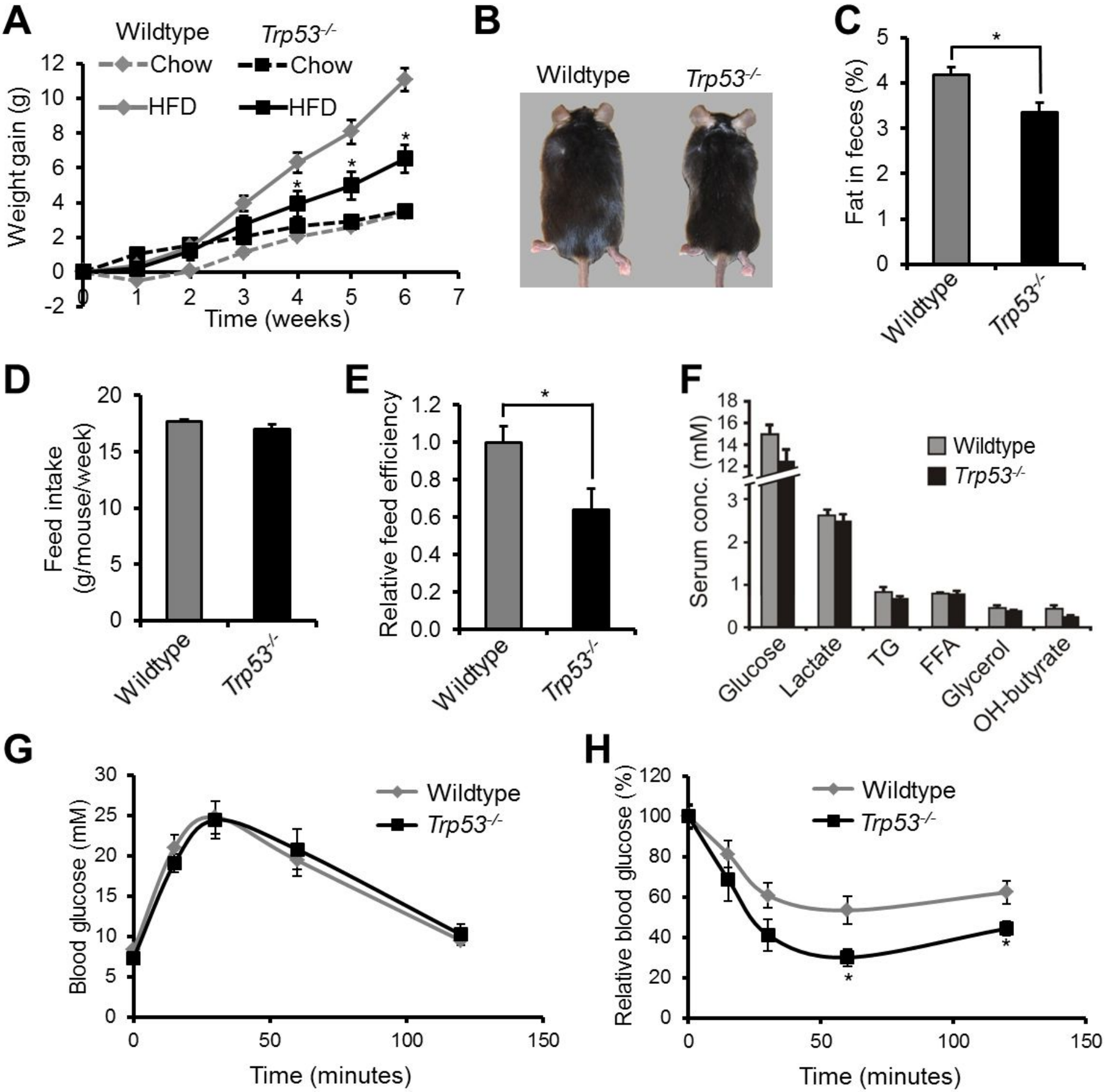
A
Wildtype
Trp53-/-
Chow
Chow
HFD
HFD
Weight gain (g)
Time (weeks)
B
Wildtype
Trp53-/-
C
Fat in feces (%)
Wildtype
Trp53-/-
D
Feed intake (g/mouse/week)
Wildtype
Trp53-/-
E
Relative feed efficiency
Wildtype
Trp53-/-
F
Serum conc. (mM)
Wildtype
Trp53-/-
Glucose
Lactate
TG
FFA
Glycerol
OH-butyrate
G
Blood glucose (mM)
Wildtype
Trp53-/-
Time (minutes)
H
Relative blood glucose (%)
Wildtype
Trp53-/-
Time (minutes)

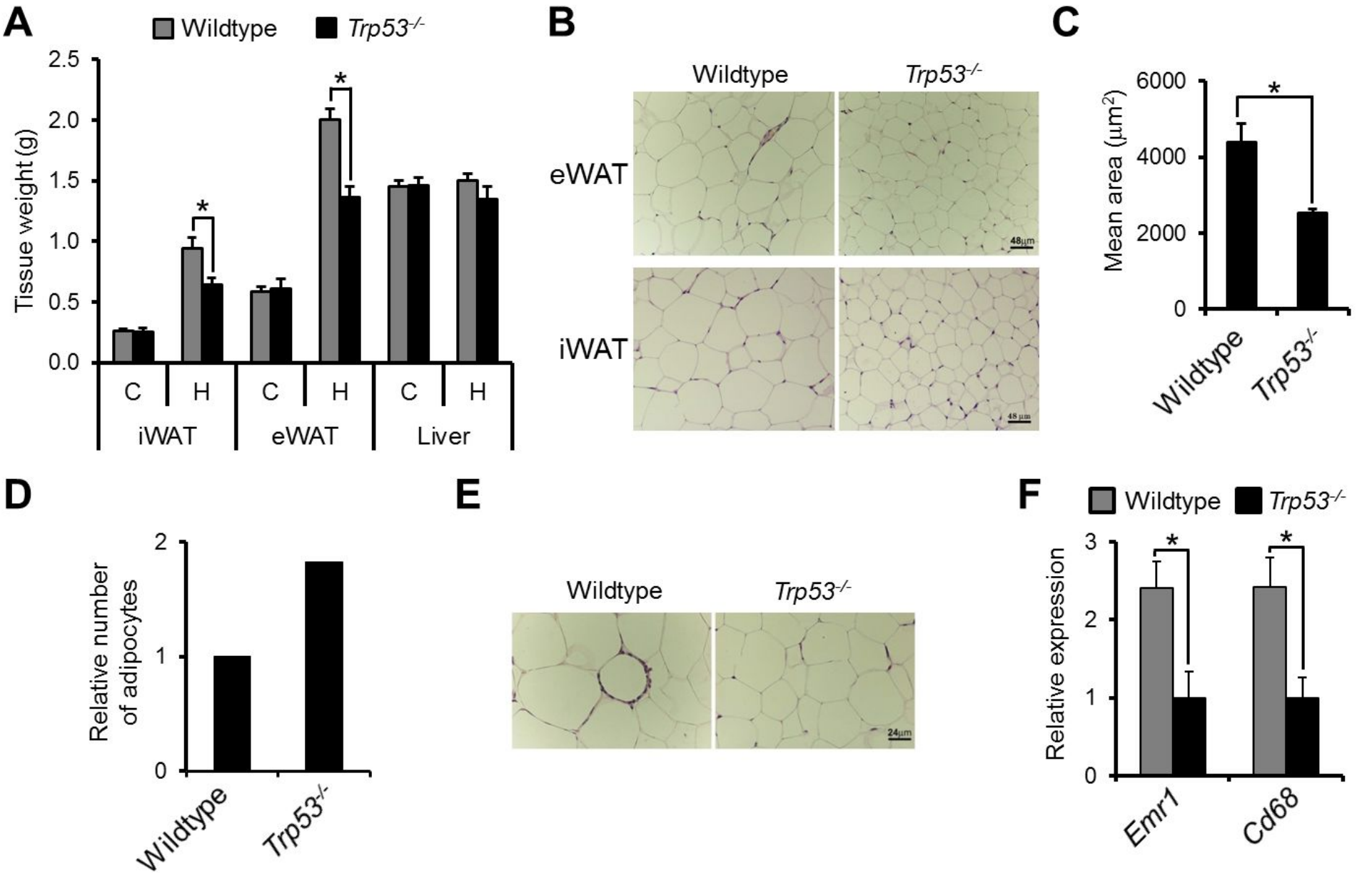
A
Wildtype
Trp53-/-
Tissue weight (g)
2.5
2.0
1.5
1.0
0.5
0.0
*
*
C
H
C
H
C
H
iWAT
eWAT
Liver
B
Wildtype
Trp53-/-
eWAT
iWAT
48μm
48 μm
C
Mean area (μm2)
6000
4000
2000
0
*
Wildtype
Trp53-/-
D
Relative number of adipocytes
2
1
0
Wildtype
Trp53-/-
E
Wildtype
Trp53-/-
24μm
F
Wildtype
Trp53-/-
Relative expression
3
2
1
0
*
*
Emr1
Cd68

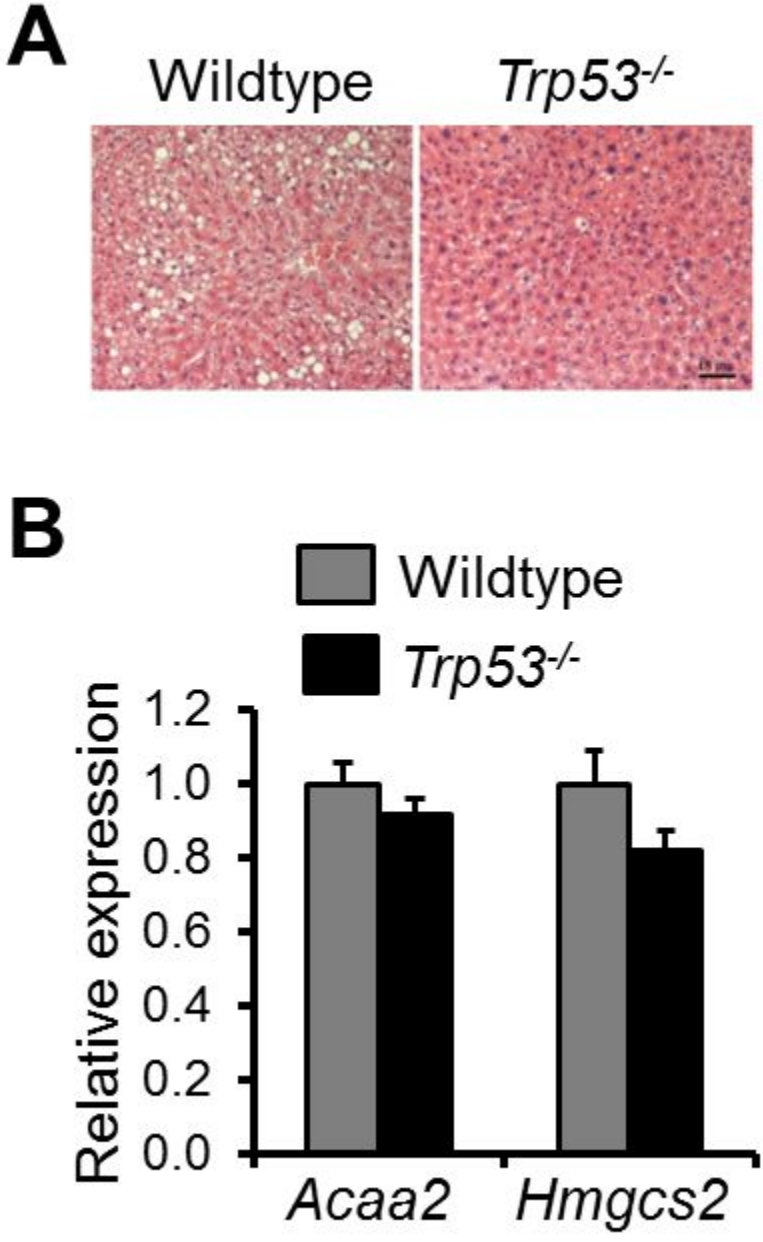
A
Wildtype
Trp53-/-
B
Wildtype
Trp53-/-
Relative expression
1.2
1.0
0.8
0.6
0.4
0.2
0.0
Acaa2
Hmgcs2

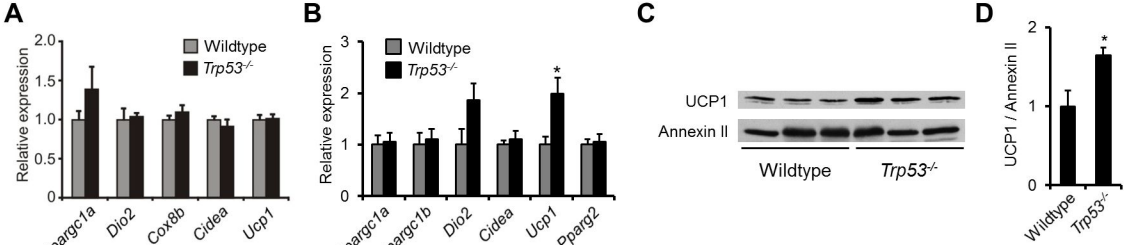
A
Relative expression
2.0
1.5
1.0
0.5
0
Wildtype
Trp53-/-
Ppargc1a
Dio2
Cox8b
Cidea
Ucp1
B
Relative expression
3
2
1
0
Wildtype
Trp53-/-
*
Ppargc1a
Ppargc1b
Dio2
Cidea
Ucp1
Pparg2
C
UCP1
Annexin II
Wildtype
Trp53-/-
D
UCP1 / Annexin II
2
1
0
*
Wildtype
Trp53-/-

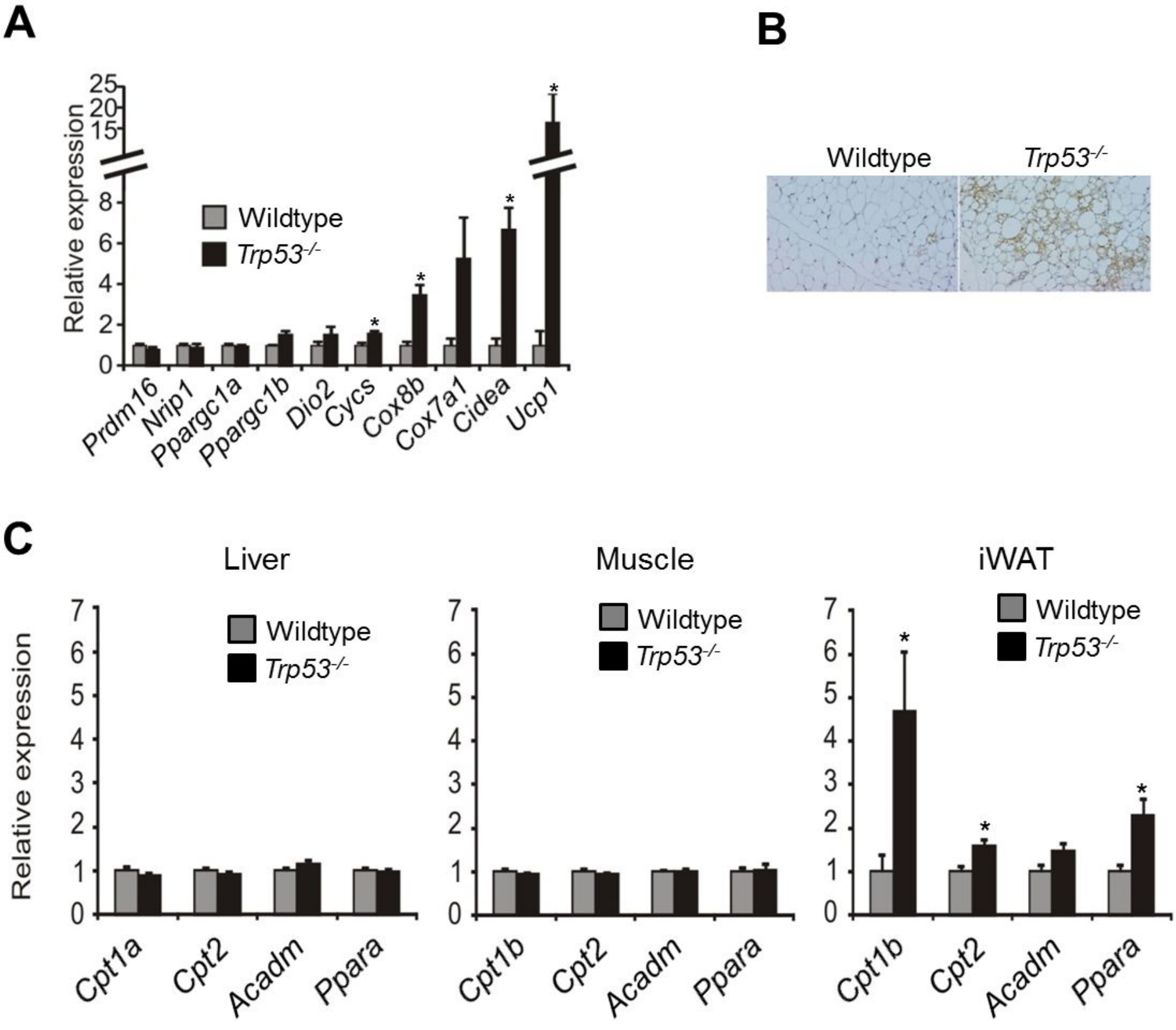
A
Relative expression
25
20
15
8
6
4
2
0
Wildtype
Trp53-/-
*
Prdm16
Nrip1
Ppargc1a
Ppargc1b
Dio2
Cycs
Cox8b
Cox7a1
Cidea
Ucp1
B
Wildtype
Trp53-/-
C
Liver
Muscle
iWAT
Relative expression
7
6
5
4
3
2
1
0
Wildtype
Trp53-/-
Cpt1a
Cpt2
Acadm
Ppara
Cpt1b
Cpt2
Acadm
Ppara

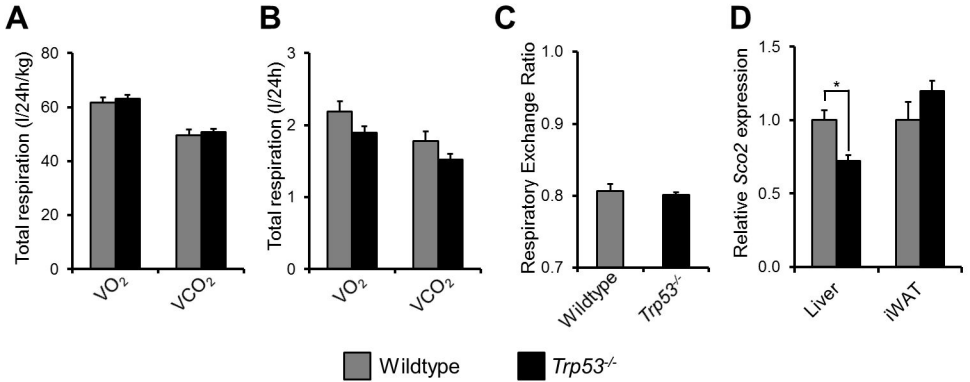
A
Total respiration (l/24h/kg)
80
60
40
20
0
VO_2
VCO_2
B
Total respiration (l/24h)
3
2
1
0
VO_2
VCO_2
C
Respiratory Exchange Ratio
1.0
0.9
0.8
0.7
Wildtype
Trp53$^{-/-}$
D
Relative *Sco2* expression
1.5
1.0
0.5
0.0
*
Liver
iWAT
Wildtype
Trp53$^{-/-}$

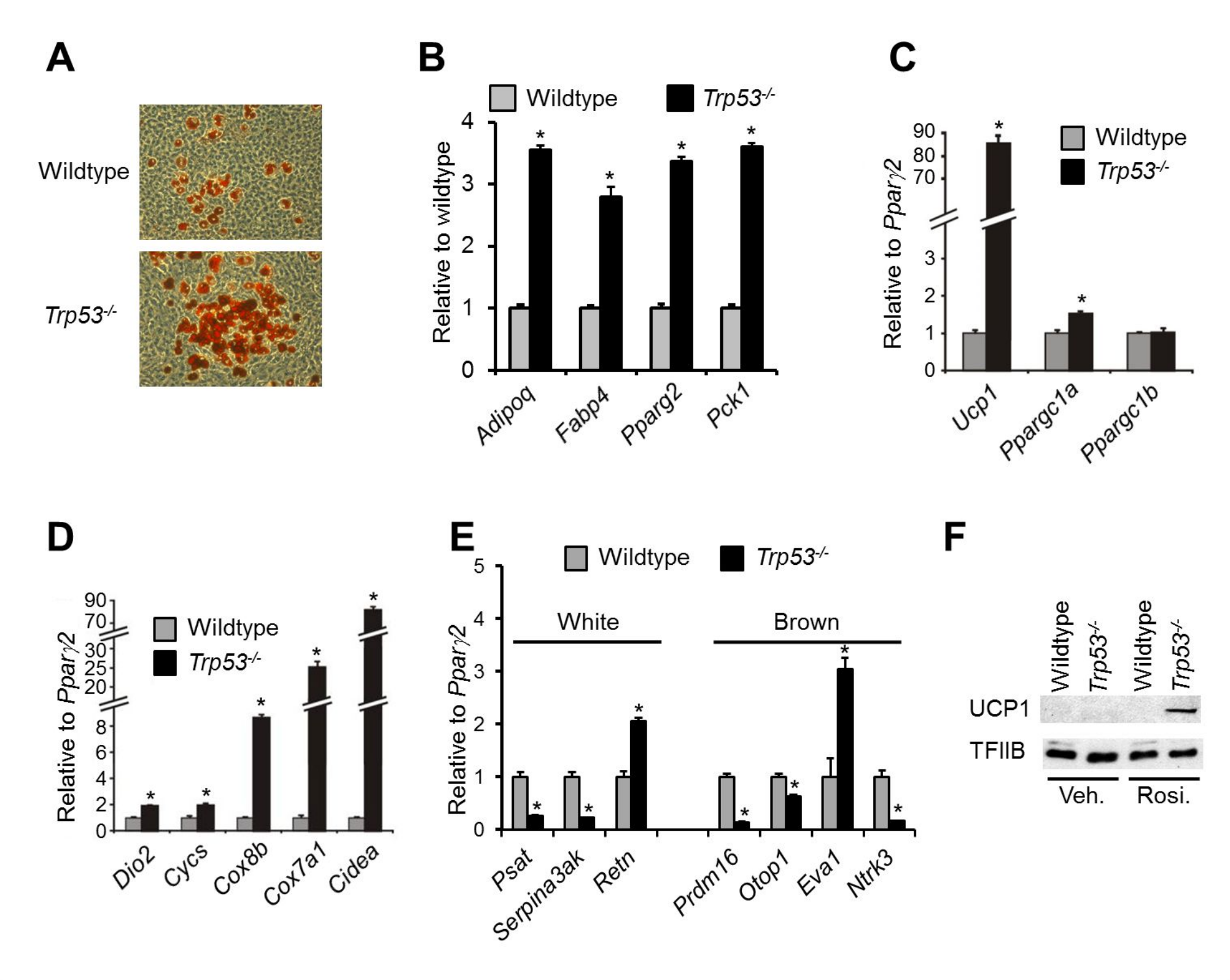
A
Wildtype
Trp53-/-
B
Wildtype
Trp53-/-
Relative to wildtype
Adipoq
Fabp4
Pparg2
Pck1
C
Wildtype
Trp53-/-
Relative to Pparγ2
Ucp1
Ppargc1a
Ppargc1b
D
Wildtype
Trp53-/-
Relative to Pparγ2
Dio2
Cycs
Cox8b
Cox7a1
Cidea
E
Wildtype
Trp53-/-
Relative to Pparγ2
White
Brown
Psat
Serpina3ak
Retn
Prdm16
Otop1
Eva1
Ntrk3
F
Wildtype
Trp53-/-
Wildtype
Trp53-/-
UCP1
TFIIB
Veh.
Rosi.

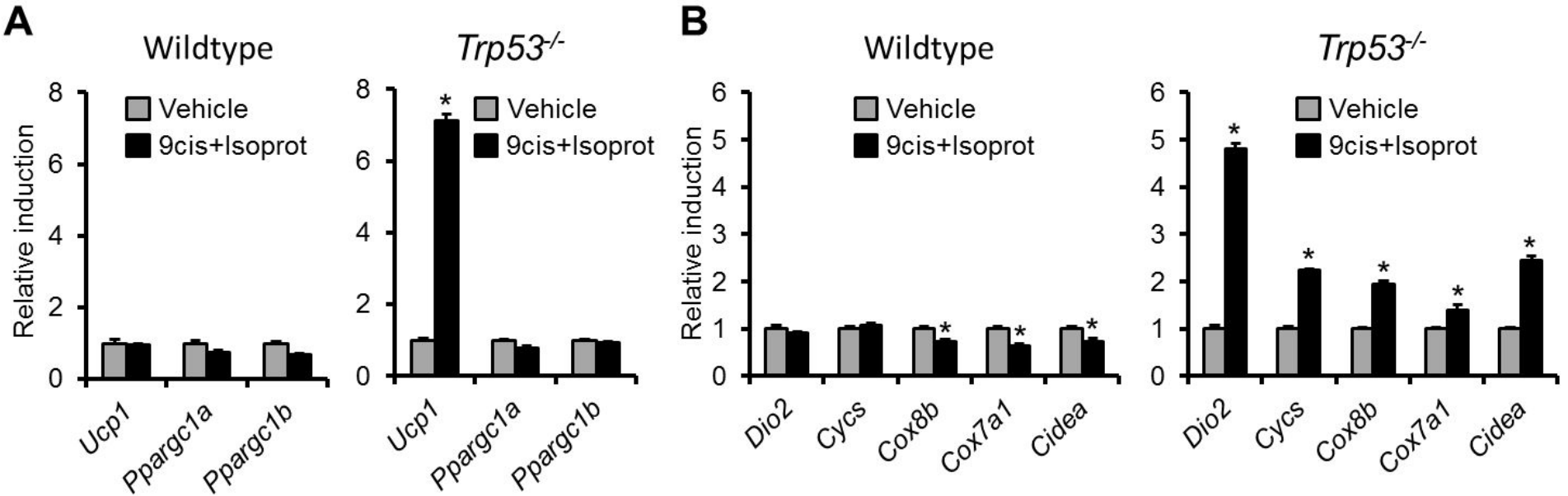
A
Wildtype
Trp53-/-
Vehicle
9cis+Isoprot
Relative induction
0
2
4
6
8
Ucp1
Ppargc1a
Ppargc1b
*
B
Wildtype
Trp53-/-
Vehicle
9cis+Isoprot
Relative induction
0
1
2
3
4
5
6
Dio2
Cycs
Cox8b
Cox7a1
Cidea
*

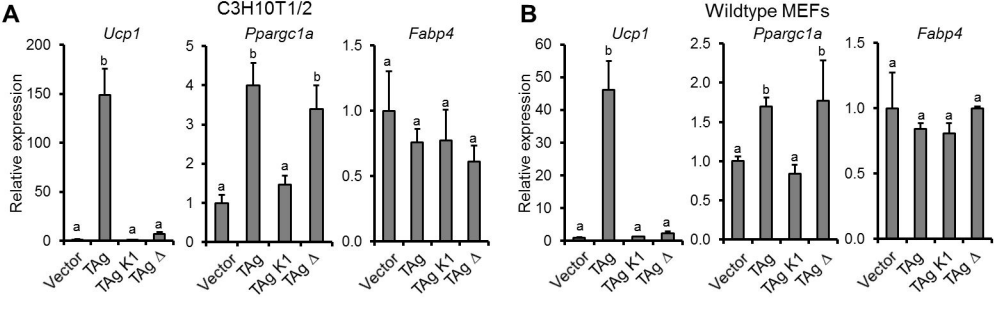
A
C3H10T1/2
Ucp1
Ppargc1a
Fabp4
Relative expression
Vector
TAg
TAg K1
TAg Δ
B
Wildtype MEFs
Ucp1
Ppargc1a
Fabp4
Relative expression
Vector
TAg
TAg K1
TAg Δ

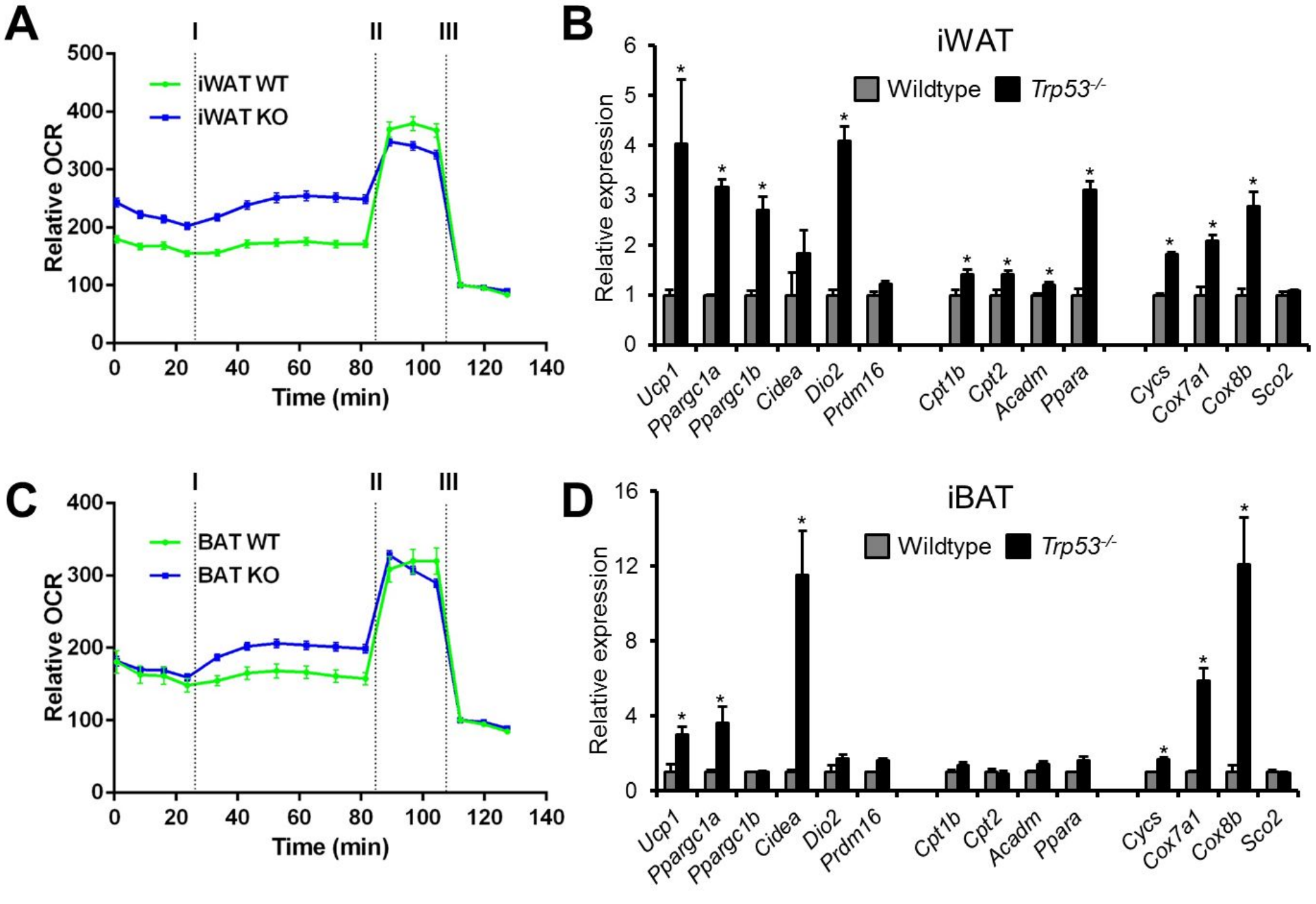
A
I
II
III
iWAT WT
iWAT KO
Relative OCR
Time (min)
B
iWAT
Wildtype
Trp53-/-
Relative expression
Ucp1
Ppargc1a
Ppargc1b
Cidea
Dio2
Prdm16
Cpt1b
Cpt2
Acadm
Ppara
Cycs
Cox7a1
Cox8b
Sco2
C
BAT WT
BAT KO
D
iBAT

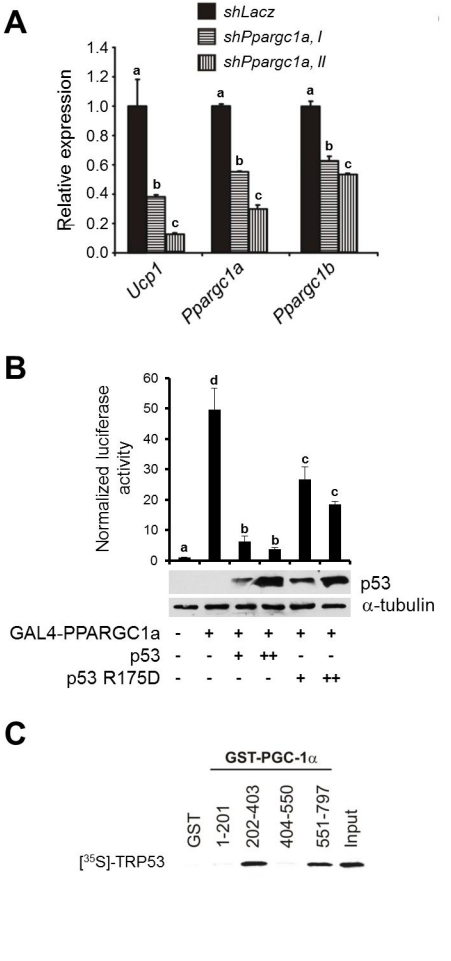
A
shLacz
shPpargc1a, I
shPpargc1a, II
Relative expression
1.4
1.2
1.0
0.8
0.6
0.4
0.2
0.0
a
b
c
a
b
c
a
b
c
Ucp1
Ppargc1a
Ppargc1b
B
Normalized luciferase activity
60
50
40
30
20
10
0
a
d
b
b
c
c
p53
α-tubulin
GAL4-PPARGC1a - + + + + +
p53 - - + ++ - -
p53 R175D - - - - + ++
C
GST-PGC-1α
GST
1-201
202-403
404-550
551-797
Input
[35S]-TRP53

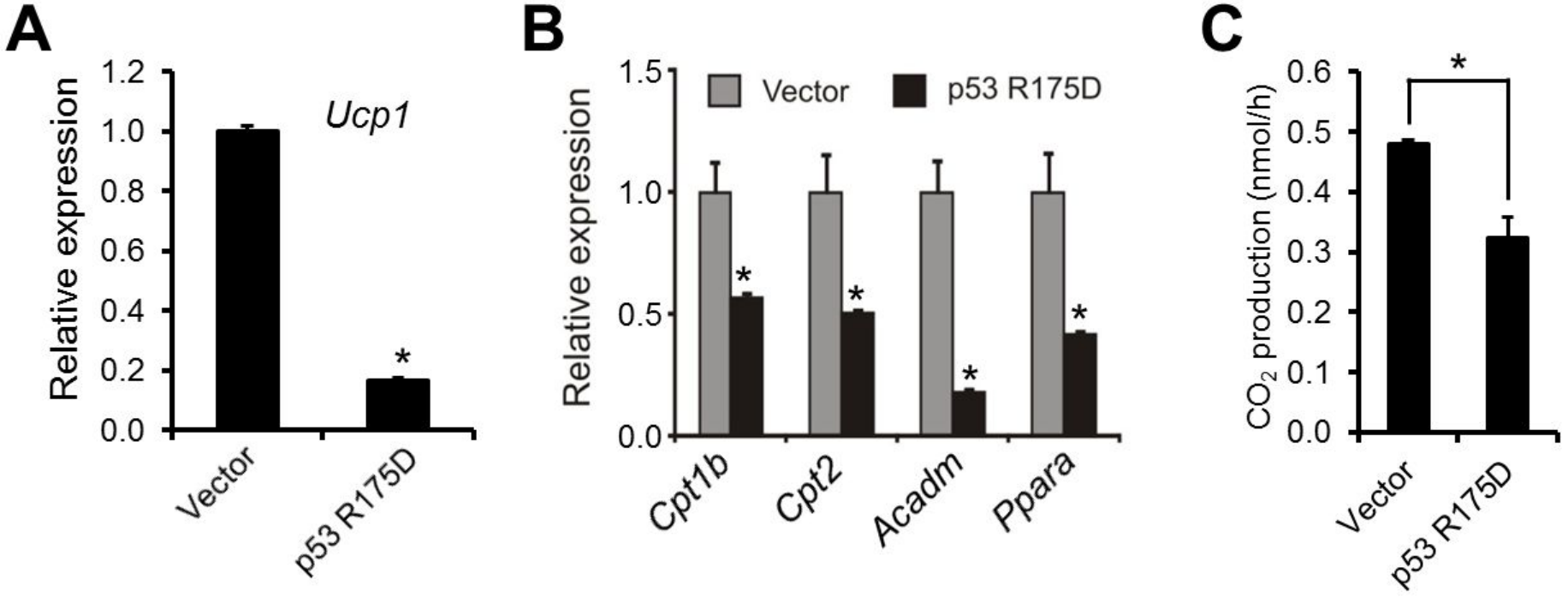
A
Relative expression
1.2
1.0
0.8
0.6
0.4
0.2
0.0
Ucp1
*
Vector
p53 R175D
B
Relative expression
1.5
1.0
0.5
0.0
Vector
p53 R175D
*
*
*
*
Cpt1b
Cpt2
Acadm
Ppara
C
CO2 production (nmol/h)
0.6
0.5
0.4
0.3
0.2
0.1
0.0
*
Vector
p53 R175D